TÉCNICO LISBOA

Comparing methodologies for evaluation of fatigue life of a highway bridge using measurement data

António Francisco Kam da Silva Andrade

Thesis to obtain the Master of Science Degree in

Civil Engineering

Supervisor: Prof. Rita Maria do Pranto Nogueira Leite Pereira Bento

Examination Committee

Chairperson: Prof. José Joaquim Costa Branco de Oliveira Pedro
Supervisor: Prof. Rita Maria do Pranto Nogueira Leite Pereira Bento
Members of the Committee: Prof. João José Rio Tinto de Azevedo

September 2017

Acknowledgements

The author would like to thank the following people that contributed towards the completion of this master thesis. Mr. Sai Pai, for his neverending patience and willingness to share his expertise. Prof. Ian Smith for his guidance and extraordinary insight on not only data-interpretation, but all matters related to structural engineering. Prof. Rita Bento for her promptness in helping me whenever I needed. My family, for always making their first priority to make it possible for me to not worry about anything else other than achieving my goals, and my friends for the constant support and encouragement.

Abstract

Structural sensing provides aditional information concerning a given structure, which can be used to improve understanding regarding its behaviour. Data gathered from sensors has to be interpreted using probabilistic data-interpretation techniques that lead to robust parameter identification, allowing updated models to be used to predict structural response at unmeasured locations. In this study, three data-interpretation techniques are compared – Residual minimization, Bayesian model updating (BMU) and Error-domain model falsification (EDMF). EDMF and BMU are first used on an illustrative example as an introductory exercise to system identification. Fatigue-life prediction for a highway bridge is made using these three techniques and results are used to evaluate robustness of these methodologies. A large bias is obtained for the predictive distrbution given by BMU. Spatial correlations between uncertainties can't be assumed as independent, or a model class containing systematic error inducing parameters has to be used in order for BMU to provide with good results. EDMF permits robust predictions to be made with a simpler model class. The simplicity in the EDMF methodology makes it a better technique to be used in applications pertaining to asset-management.

Keywords : Model-based data-interpretation ; Residual minimization ; Bayesian model updating ; Model falsification ; Full scale structures

Resumo

A monitorização de uma estrutura através de sensores permite a obtenção de informação adicional, que pode ser usada para melhor compreender o seu comportamento. Esta informação tem de ser interpretada com recurso a metodologias probabilísticas que levam a uma identificação robusta de parâmetros estruturais, de modo a permitir a utilização de modelos actualizados para previsão de comportamento estrutural em locais não monitorizados. Neste trabalho, uma comparação é feita entre três metodologias de interpretação de dados – *Residual minimization, Bayesian model updating* (BMU) e *Error-domain model falsification* (EDMF). Em primeiro lugar, o EDMF e o BMU são aplicados a um exemplo teórico como exercício introdutório à identificação estrutural. De seguida, as três metodologias são usadas para a previsão da vida útil em fadiga de uma ponte rodoviária e os resultados são comparados de modo a avaliar a robustez de cada metodologia. Os resultados obtidos através do BMU apresentam grande enviesamento. Para obter resultados fidedignos com o BMU as incertezas não podem ser consideradas como independentes, ou o conjunto de parâmetros a identificar tem de conter parâmetros que induzem erros sistemáticos. Os resultados obtidos com o EDMF são robustos e esta metodologia permite a utilização de um conjunto de parâmetros mais simples para a identificação estrutural. A simplicidade na utilização e interpretação do EDMF confere à metodologia uma maior compatibilidade com aplicações práticas de gestão de infraestruturas.

Palavras-chave : Interpretação de dados com base em modelos ; Identificação Bayesiana ; Falsificação de modelos ; Estruturas em tamanho real

Contents

List of Figures

List of Tables

Notation

BMU - Bayesian model updating

CAFL - Constant amplitude fatigue limit

CD1 - Critical detail 1

CD2 - Critical detail 2

CD3 - Critical detail 3

D - Damage index

E - Young's modulus

EDMF - Error-domain model falsification

FEM - Finite element model

FAT - Fatigue category for a detail

g - Model precitctions

G - Model Class

GUI - Graphical user interface

I - Moment of inertia

K - Spring stiffness

KDECKX - Connection of the Venoge bridge’s concrete deck and steel girders longitudinally

KDECKZ - Connection of the Venoge bridge’s concrete deck and steel girders transversally

KYO - Vertical stiffness of support 0 of the Venoge bridge

KXO - Horizontal stiffness of support 0 of the Venoge bridge

ROTZO - Rotational stiffness of support 0 of the Venoge bridge

KY1 - Vertical stiffness of support 1 of the Venoge bridge

KX1 - Horizontal stiffness of support 1 of the Venoge bridge

L - Length

R - Structural response

SB - Sensor location B

SC - Sensor location C

Sup 0 - Support 0 of the Venoge bridge, as given by Figure 7

Sup 1 - Support 1 of the Venoge bridge, as given by Figure 7

Sup 2 - Support 2 of the Venoge bridge, as given by Figure 7

Sup 3 - Support 3 of the Venoge bridge, as given by Figure 7

Sup 4 - Support 4 of the Venoge bridge, as given by Figure 7

m - Slope of the S-N curve

MH - Metropolis-Hastings

MLE - Maximum likelihood estimate

N - Number of load cycles to failure

n_m - Number of measurements

PDF - Probability density function

q - Realization of the prediction quantity

RFL - Remaining fatigue life

SIA - Swiss code for design and construction in Switzerland (Swiss Society of Engineers and Architects)

S-N - Graph of the magnitude of a cyclic stress (S) against the logarithmic scale of cycles to failure (N)

T - Threshold bound

w - Weighing factor

WIM - Weigh in motion

x - Longitudinal coordinate for the beam example presented on chapter 3

y - Measured value

U - Uncertainty source described by a random variable

f_U - Probability density function describing a random variable U

$\Delta\sigma$ - Stress range

$\Delta\sigma_c$ - Reference stress range value

$\Delta\sigma_D$- Threshold stress range for crack propagation

β - Regression coefficients

δ - Displacement

θ - Parameter vector to indentify

θ^* - True parameter vector

$\hat{\theta}$ - Optimal parameter vector

Θ - Parameter domain

ϕ - Target identification reliability

μ - Mean

σ - Standard deviation

ε - Error

1. Introduction

1.1 Problem statement

Three data-interpretation techniques are used in this work to predict remaining fatigue life (RFL) of a highway bridge. The results are analysed to evaluate the robustness of each method for parameter identification. With advances in structural sensing, an everlasting built environment is now achievable in the foreseeable future. To attain such conjuncture, sensor data has to be interpreted in an accurate and robust manner, thus enabling efficient infrastructure management through appropriate inspection, maintenance and repair. Civil engineering infrastructures are designed using conservative models. Therefore, they possess reserve capacity that can be explored to make them last beyond their design life. Sensor information regarding a structure can be used to reduce model uncertainty and estimate this reserve capacity (Pasquier and Smith 2016). However, a methodology that makes rigorous treatment of modeling uncertainty and that is robust to incomplete knowledge is needed in order to make accurate predictions regarding reserve capacity of a structure.

Several data-interpretation techniques used presently are based on assumptions that are not necessarily applicable in the context of civil engineering. Two of these most commonly used techniques - residual minimization and Bayesian Model Updating (BMU) – are used in this study alongside a novel methodology proposed by Goulet and Smith (2013) – Error-domain model-falsification (EDMF) - for fatigue life predictions and a comparison is made regarding prediction accuracy and robustness. Models are, by definition, approximations of reality. Simplifications regarding geometry, material properties, etc. induce bias in the model, while innapropriate model forms, simplified boundary conditions and other assumptions lead to errors that are systematic and spatially correlated. Pasquier and Smith (2015) presented several examples of common sources of uncertainty that arise from assumptions made when modeling complex civil engineering structures. In order to obtain accurate indentification, the employed methodology has to be robust when in presence of these uncertainties.

Studies have been made showing that commonly used techniques such as residual minimization and Bayesian model updating can lead to biased results due to the misevaluation of the modeling error's probability density function (PDF) and their spatial correlations (Goulet and Smith 2013; Simoen et al. 2013; Pasquier and Smith 2015). Moreover, Yan and Katafygiotis (2015) noted that civil engineering structures might not be identifiable in a Bayesian framework due to their complex nature and high number of parameters. These outcomes can therefore lead to misguided asset-management decision-making. A methodology that is not only robust in the presence of varying uncertainty, but that also permits accurate predictions while using reduced models is then needed. Goulet and Smith (2013) proposed an approach that makes a combination of each source of uncertainty and falsifies inadequate models based on conservative probabilistic thresholds computed on an estimated PDF of these combined uncertainties. This is an approach that leads to robust identification of parameters without the need of precise knowledge about modelling error dependencies.

Even though comparisons between data-interpretation techniques have been made on illustrative examples, where it has been demonstrated that, when utilizing a Bayesian approach and in the presence of systematic errors, biased posterior distributions can be obtained due to assumptions of independence between uncertainties (Goulet and Smith 2013; Pasquier and Smith 2015; Simoen et al. 2013), few studies have been conducted on real structures. Pai et al. (2017) evaluated the applicability of EDMF, BMU and modified BMU in the prediction of the remaining fatigue life (RFL) of a cover plate detail of the Venoge bridge, located in Switzerland. Results showed that both EDMF and modified BMU give robust bounds that include the value obtained from measurements, for RFL prediction of the cover plate detail.

The techniques used in data-interpretation require a large number of simulation runs using a finite element (FE) model of the structure, which is computationally expensive. One way of bypassing this time-consuming process is to build surrogate models to replace the finite element model. There are various methodologies that can be used to build surrogate models. Some of them have been reviewed by Rutherford et al. (2006). Neural networks are used in this study to predict structural response for fatigue life assessment.

This dissertation work builds on the research carried out by Pai et al. (2017) through studying and comparing the robustness of three data-interpretation techniques – residual minimization, BMU and EDMF – to variations in modeling error and selection of model class. Different scenarios regarding uncertainty estimation are considered and the difference in results for each methodology is studied using a graphical user interface (GUI) toolbox developed. A different model class from the one used in Pai et al. (2017) is adopted and disparities in results are compared. RFL for three different critical details is also predicted using updated information of the Venoge bridge.

1.2 Objectives

The objectives for this thesis are the following :

- Determine sources and forms of uncertainty for identification of structural parameters and prediction of structural response.
- Determine model classes that describe structural behavior at measurement locations.
- Evaluate and compare applicability of residual minimization, BMU and EDMF for interpretation of measurement data to improve understanding of structural behavior.
- Estimate reserve capacity of the structure using updated knowledge of structural behavior.
- Develop methods to aid in decision-making pertaining to asset-management.

1.3 Structure

This document follows the following structure :

- Section 2 – A description of the data-interpretation methodologies used in this study is made.
- Section 3 – EDMF and BMU are applied to an illustrative example.
- Section 4 – Results for structural identification of a real structure – the Venoge bridge - using three different methodologies are presented and validated for two measurement locations that were not used for updating. Remaining fatigue life predictions are made for three critical details.
- Section 5 – A toolbox developed to assess the robustness of each methodology and aid in decision-making is described.
- Section 6 – Considerations regarding the presented results are made.
- Section 7 – Final conclusions are listed.

2. Methodologies of data-interpretation

In this chapter, a brief explanation of the three data-interpretation methodologies – residual minimization, BMU nad EDMF – is presented.

2.1 Residual minimization

One of the most commonly used data-interpretation techniques is residual minimization. The methodology focuses on finding a parameter vector θ that minimizes sum of the square of the residual difference between model predictions $g_i(\theta)$ and measured values y_i at every measurement location $i = \{1, \dots, n_m\}$:

$$\hat{\theta} = \arg min \sum_{i=1}^{n_m} w_i \, (g_i(\theta) - y_i)^2 \tag{1}$$

where $\hat{\theta}$ contains the optimal parameter values, n_m is the number of measurement locations and w_i are weighting factors. As suggested by Mottershead et al. (2011), $w_i = y_i^{-2}$ is used in this study. The parameter values $\hat{\theta}$ are optimal if the residual between predictions and measurements follow a zero-mean independent Gaussian distribution. This assumption is often not satisfied in civil engineering structures, given that a model $g(\theta)$ merely approximates the behavior of a structure and, as noted by Mcfarland and Mahadevan (2008), independence between uncertainties is seldom verified.

2.2 Bayesian model updating

Bayesian model updating (BMU) is a method that uses Bayes' theorem to update the prior knowledge of model parameters using available information (i.e. measurements). The prior distribution $P(\theta)$ of the unknown parameters of the model is updated using a likelihood function $P(y|\theta)$ according to Bayes theorem :

$$P(\theta|y) = \frac{P(y|\theta)P(\theta)}{P(y)} \tag{2}$$

In Eq. 2 $P(y)$ represents the normalization constant and $P(\theta|y)$ he posterior distribution. The prior knowledge expresses initial belief regarding values of structural parameters, before taking measurements into account. The likelihood gives the plausibility of observing measurement data from the model class given a specific set of parameters, and is mostly based on a Gaussian distribution, as shown in Eq.3.

$$P(y|\theta) \propto const. \exp\left(-\frac{1}{2}(g(\theta) - y)^T \Sigma^{-1} (g(\theta) - y)\right) \tag{3}$$

In Eq. 3 $g(\theta)$ represents a vector of model predictions, y a vector of measurement data and ∑ a covariance matrix with correlations between uncertainties at measured locations. The posterior distribution $P(\theta|y)$ is obtained using the normalization constant, $P(y)$, that can be computed by the following expression :

$$P(y) = \int_{\Theta} P(y,\theta)d\theta = \int_{\Theta} P(y|\theta)P(\theta)d\theta \quad (4)$$

where Θ is the parameter domain.

In most applications of BMU, uncertainties are usually described by independent Gaussian distributions (Beck and Katafygiotis 1998). Additionally, the same variance is assumed for every location, which is hardly the case for models that possess systematic errors. These are common assumptions made, when a Bayesian framework is applied, that can lead to biased predictions (Pasquier and Smith 2015). To obtain accurate predictions with BMU, spatial correlations have to be taken into consideration and estimated correctly, which is a hard and often unfeasible task (Simoen et al. 2013).

2.3 Error-domain model falsification

Let $g(\theta)$ be a vector of structural response predictions at various measurement locations using a model class that takes n_p physical parameters, θ_k , as an argument. If the real value of the system's parameters θ^* are known, the true response of the system is equal to the difference between the prediction given by the model $g(\theta^*)$ and the modeling error ε_{model} , and also to the difference between the measured value and the measurement error $\varepsilon_{measure}$:

$$g_i(\theta^*) + \varepsilon_{model,i} = y_i + \varepsilon_{measure,i} \quad (5)$$

In reality, the true value of the parameters as well as errors and uncertainties are unknown, and can only be described by random variables U_{model} and $U_{measure}$, each represented by probability density functions $f_U(\varepsilon)$. Eq. 5 is then written in the following form :

$$g_i(\theta) + U_{model,i} = y_i + U_{measure,i} \quad (6)$$

By rearranging the terms in Eq. 6, the following relation is obtained :

$$g_i(\theta) - y_i = U_{measure,i} - U_{model,i} \quad (7)$$

where the residual of the difference between predicted and measured values is described by a combined PDF representing modeling and measurement uncertainties.

A model instance (i.e. a combination of a model class and a parameter set) is falsified if its observed residual lies outside the interval defined by threshold bounds T_{low} and T_{high} computed over this combined PDF for a given target reliability ϕ.

$$\forall i \in [1, \dots, n_m], \qquad T_{low,i} \leq g_i(\theta) - y_i \leq T_{high,i} \quad (8)$$

$$\forall i \in [1, \dots, n_m], \quad \phi^{\frac{1}{n_m}} = \int_{T_{low,i}}^{T_{high,i}} f_{U_{c,i}}(\varepsilon_{c,i}) d\varepsilon_{c,i} \tag{9}$$

Eq. 9 gives the shortest interval [T_{low} T_{high}] over the combined ucertainty PDF for each measurement location $f_{U_{c,i}}(\varepsilon_{c,i})$ that contains the target reliability ϕ. The Šidák (Šidák 1967) correction is used, which leads to the determination of conservative bounds without having to take into account correlations between uncertainties (Goulet and Smith 2013).

Model instances that are not falsified are considered as candidate models and all instances are equally likely to explain observed behavior. A model class G is falsified when all its model instances are falsified by these threshold bounds. When a model class is falsified, a review on initial assumptions is suggested. Predictions q_j can then be made by combining distributions of candidate model predictions $g_j(U_{\theta^*})$ with distributions of modelling error for each prediction location j.

$$q_j = g_j(U_{\theta^*}) + U_{model,j} \tag{10}$$

The EDMF methodology has been applied to several case studies since its proposal. A list of these applications can be found in Smith (2016).

3. Illustrative example

In this chapter, a preliminary study is done as an introductory exercise to structural identification. EDMF and BMU are used to identify the parameters of a simple structure. The illustrative structure consists of a cantilever beam, where the rotation of the fixed end is modeled by a rotational spring of stiffness K, as presented in Figure 1.

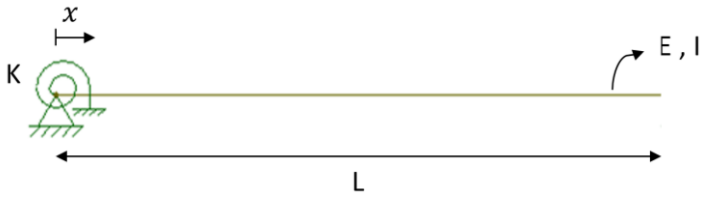

Figure 1 Illustrative structure to which data interpretation methods will be applied

The beam has a rectangular cross section of inertia I, and the other parameters that characterize its linear structural behavior are its length L, the Young's modulus E, and the rotational stiffness K. The true values set for these parameters are presented on Table 1. The beam's displacement $\delta(x)$ at a given location x due to a force F applied on its free end can be calculated using the following expression:

$$\delta(x) = \frac{F}{EI}\left(\frac{x^3}{6} - \frac{Lx^2}{2}\right) - \frac{FL}{K}x \tag{11}$$

Three measurement locations are used, where simulated measured displacements $y_i(x)$ are obtained by adding to the real displacement $\delta^*(x)$ a measurement error that follows a zero mean Gaussian distribution with a standard deviation of 0.02 mm. The measurement coordinates x_i are taken between $x = x_s = 5000\ mm$ and $x = L - x_s$ and are given by:

$$x_i = x_s + (L - 2x_s)\frac{i}{n_m + 1} \tag{12}$$

With n_m being the number of measurements, which in this example is equal to three. The possible ranges of values for the beam's parameters are described in the following Table:

	E $[\boldsymbol{GPa}]$	**L** $[\boldsymbol{mm}]$	**K** $[\boldsymbol{Log(Nmm/rad)}]$	**I** $[\boldsymbol{mm^4}] \times \boldsymbol{10^8}$	**F** $[\boldsymbol{kN}]$
True value	31	8100	11	54.20	20
Initial parameter range	30 - 40	8000 - 8500	9 - 12	52 – 56	20

Table 1 True values and initial ranges for the beam's parameters.

3.1 Sensitivity analysis

In order to select the model class for identification, a sensitivity analysis was conducted to study the parameters that have the most influence on the beam's response. A simple linear regression sensitivity analysis was carried out for each of the three measurement locations. Engineering judgment is used to first define initial beliefs regarding parameters that affect structural response at measurement locations. These parameters and the initial range of values considered for them are presented in Table 1. In order to study the response of the beam to the variation of these parameters, a linear regression was made of the beam's response computed over a Box-Behnken design (Box and Behnken 1960) of the structural parameters, for each measurement location.

$$R = \beta_1\theta_1 + \beta_2\theta_2 + \cdots + \beta_k\theta_k \tag{13}$$

In Eq. 13 structural response R is expressed as a linear combination of the structure's parameters θ_k. The regression coefficients β_k can be interpreted as weights that indicate the relative importance of a given parameter in structural response. A more detailed description of the procedure taken for the sensitivity analysis can be found in Appendix A.

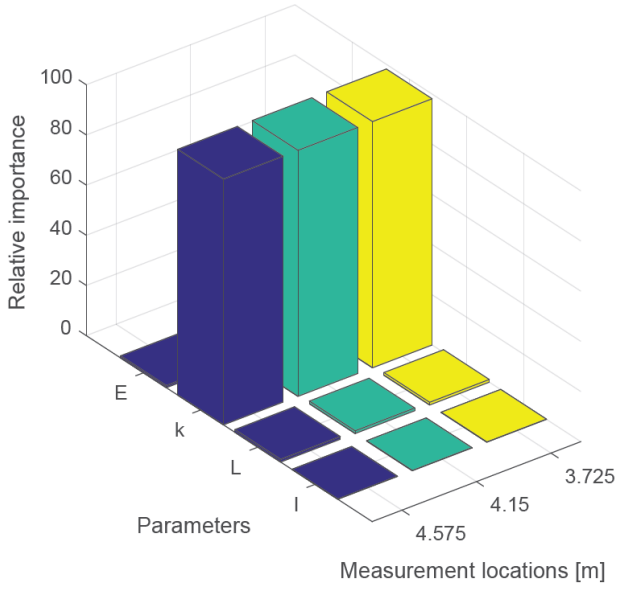

Figure 2 Influence of each individual parameter on the beam's displacement

By analysing the results presented in Figure 2, it can be seen that the most dominant parameter, when it comes to influence over the beam's displacement, is the rotational stiffnes K of the beam's spring. These results are obtained due to the wide initial range of values taken for K, and also due to the rotational spring being the only element governing the boundary conditions of the beam. Given these results, the model class selected for this example is composed solely by the parameter K.

3.2 Results obtained from error-domain model falsification

By not including the other three parameters in the model class, secondary parameter uncertainty has to be quantified. Since the true displacement of the beam for every measurement location is known, the error can be computed by :

$$\varepsilon_{II}(\%) = \frac{\delta^* - \delta_{II}}{\delta^*} \times 100 \tag{14}$$

Where ε_{II} represents the secondary parameter error, δ^* is the true displacement of the beam and δ_{II} the displacement of the beam computed using a given set of values for the secondary parameters and the true value K^* of the spring's rotational stiffness. If a large enough sample for δ_{II} is taken, where the values of the secondary parameters are varied, the mean and standard deviation for the distribution of ε_{II} can be calculated. The error, represented in millimiters, can then be obtained by multiplying the values of ε_{II} by the true value of the beam's displacement. By the principle of maximum entropy a Gaussian distribution is used to describe secondary parameter uncertainty.

As mentioned in chapter 3, sensor noise following a zero mean Gaussian distribution was added to the true value of the beam's displacement in order to simulate measurements. Since all the uncertainties follow Gaussian distributions, the mean and variance of the combined uncertainty PDF describing the observed residuals can be obtained by simply subtracting the mean and adding the variance of the secondary parameter uncertainty for the given location to the Gaussian sensor noise. The mean and standard deviations obtained for the combined uncertainty PDF in each location are described in Table 2.

	$x_1 = 4575\ mm$	$x_2 = 4150\ mm$	$x_3 = 3725\ mm$
Mean (mm)	0.56	0.49	0.42
Standard deviation (mm)	1.92	1.68	1.44

Table 2 Mean and variance for combined uncertainty PDF for each measurement location.

Since the combined uncertainty PDF follows a Gaussian distribution, the inverse cumulative distribution function is used to compute the threshold bounds. The bounds were obtained for a target reliability $\phi = \sqrt[3]{0.95}$ since three measurement locations are being taken.

	$x_1 = 4575\ mm$	$x_2 = 4150\ mm$	$x_3 = 3725\ mm$
$T_{low}\ (mm)$	-4.0347	-3.5175	-3.0228
$T_{high}\ (mm)$	5.1475	4.4876	3.8565

Table 3 Threshold bounds for each measurement location.

After obtaining the threshold bounds, 10 000 samples of K were taken. Model instances whose residuals did not fall within the domain defined by the bounds were falsified and the remaining ones are all considered as

candidate models. Out of the initial 10 000 model instances, 8238 were rejected and 1762 candidate models were found. The range of K of the accepted model instances are shown in Figure 3.

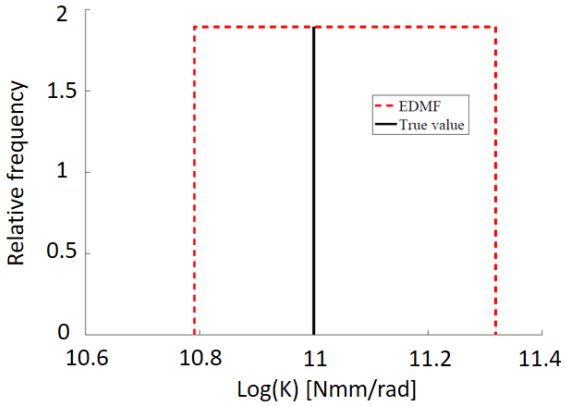

Figure 3 Range of values for K accepted by EDMF

3.3 Results obtained from Bayesian model updating

For BMU, the ranges presented in Table 1 define uniform distributions that are updated with a likelihood function based on an Gaussian distribution centered on the mean value of the combined uncertainty PDF. Spatial independency was assumed between measurement locations, so the covariance matrix for the likelihood function is a diagonal matrix where in each element of the diagonal lies the variance of the combined uncertaint PDF for each measurement location σ_i^2.

$$\Sigma = \begin{bmatrix} \sigma_1^2 & 0 & 0 \\ 0 & \sigma_2^2 & 0 \\ 0 & 0 & \sigma_3^2 \end{bmatrix} = \begin{bmatrix} 3.70 & 0 & 0 \\ 0 & 2.81 & 0 \\ 0 & 0 & 2.08 \end{bmatrix} \quad [mm]$$

The range set for the values of K define a uniform distribution as the prior distribution for the rotational spring's stiffness. Taking three measurement locations means that the integral of the normalization constant presented in Eq. 4 is three dimensional, which is difficult to compute. To get around having to compute Eq. 4 by direct numerical integration, 100 000 samples of the posterior distribution were taken using Markov Chain Monte Carlo simulation based on the Metropolis-Hastings algorithm, with verified convergence. It has been shown, in the context of civil engineering, that the samples taken from the likelihood function using Markov Chain Monte Carlo based on the Metropolis-Hastings algorithm converge to the posterior distribution (Beck and Au 2002). The obtained posterior distribution is presented in Figure 4, alongside with the results of the identification using EDMF.

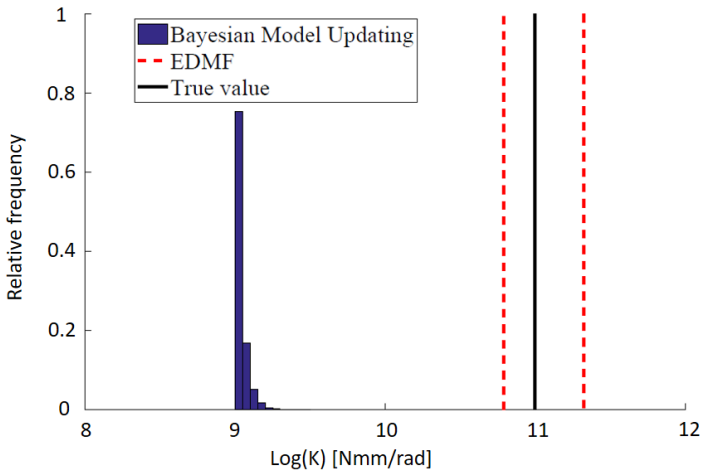

Figure 4 Summary of results from parameter identification using EDMF and Bayesian Model Updating

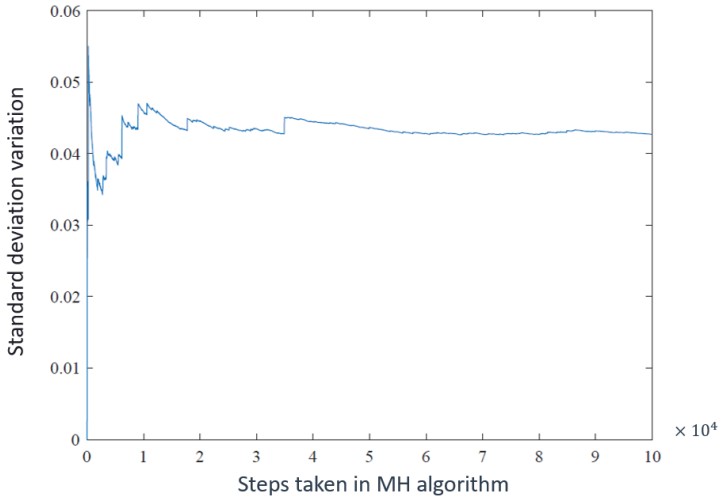

Figure 5 Variation of the standard deviation for every step taken in the Markov chain

Figure 4 shows that Bayesian model updating led to biased identification of the value of K. By interpreting Figure 5, where the variation of the posterior distribution's standard deviation for every step taken in the Markov chain is plotted, it can be seen that the Markov chain indeed converges. Thus, the biased results are due to wrongly assumed spatial correlation values between measurement locations. The same conclusion was demonstrated by Pasquier and Smith (2015).

3.4 Considerations regarding the illustrative example

For the illustrative example considered herein, biased results were obtained when using Bayesian model updating for identification of a single parameter, whereas EDMF led to correct parameter identification. In a purely academic study, where the true value of the structure's parameters are known, it is easy to quantify uncertainties, obtain results and compare methodologies. In a real structure, where little is known about modelling errors, such tasks are hard to achieve. Nonetheless, there is still the need to compare and evaluate the applicability of

different data-interpretation techniques using full scale structures, as results obtained severely influence decision-making. In the next chapter, three techniques are compared for fatigue life evaluation of a real highway bridge.

4. Case study

4.1 Structure description

The structure considered in this study, called as the Venoge bridge, is a 219m net span steel-concrete composite bridge located in the municipality of Denges, Switzerland. The bridge is part of the swiss A1 highway that connects the cities of Lausanne and Geneva. It was originally built in 1961, with two identical independent bridges, one for each direction of the motorway. In 1995, the bridge was extended to accomodate an extra lane in each direction. The old and extended part of the bridge are indicated in Figure 6. The extended part of the bridge is studied in this work, as it is the location of the slow lane on which heavy vehicles pass.

Figure 6 Old and extended sections of the Venoge bridge

The concrete deck is supported by four girders in each direction, where both the old part of the bridge and the extension are supported by two girders each. The bridge is divided into four spans with the dimensions shown in Figure 7. The five supports are referred as Sup 0, Sup 1, Sup 2 and Sup 4 throughout this dissertation. There is a total of 39 stiffeners (*200x55mm*) distributed along each girder, and 25 transversal beams located along the bridge. Fatigue life predictions are made for three different details in this study :

- Critical detail 1 (CD1), located 26m from the Lausanne abutment
- Critical detail 2 (CD2), located 112m from the Lausanne abutment
- Critical detail 3 (CD3), located 139.5m from the Lausanne abutment

The Venoge bridge is monitored with twelve sensors distributed over two sections in the first span. The location of the sensors and the critical details studied in this work are presented in Figure 7.

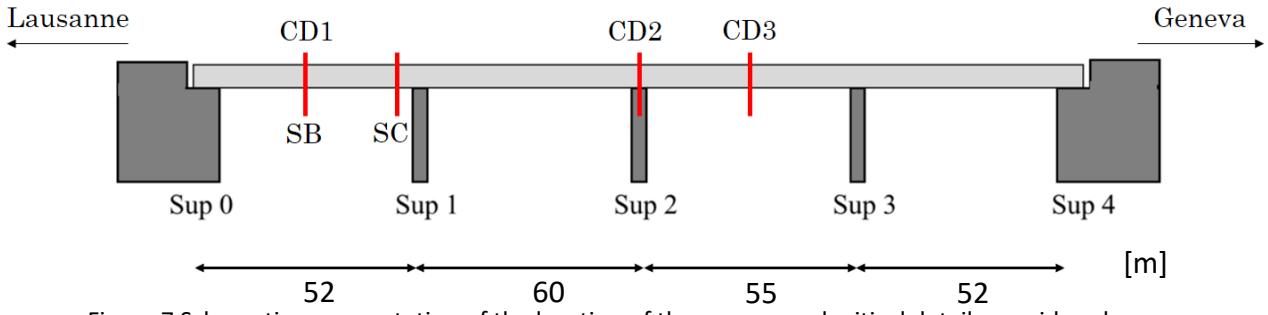

Figure 7 Schematic representation of the location of the sensors and critical details considered

In Figure 7, SB and SC indicate sensor locations B and C, respectively. For each of these locations there are 6 sensors distributed over the top and bottom flanges of the interior girder that supports the extended part of the bridge. A representation of the sensor positions can be seen in Figure 8. In Figures 9 and 10 sensors located on the bottom flange of the girder can be seen.

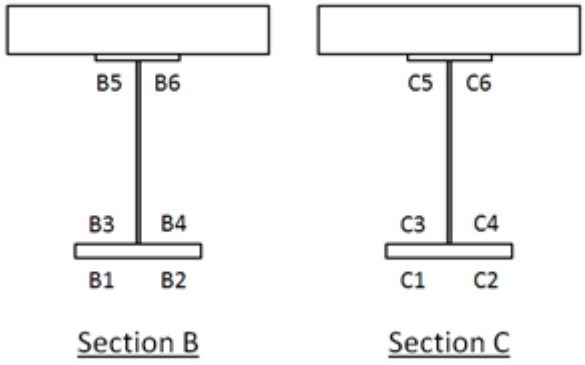

Figure 8 Location of the sensors

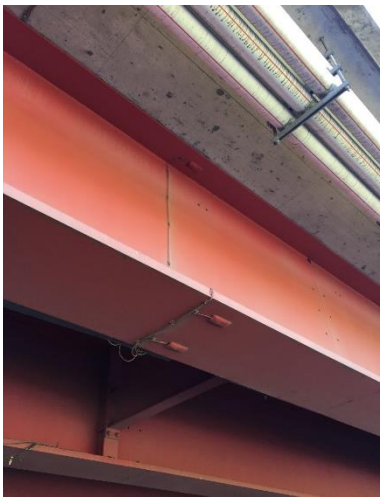
Figure 9 Sensor location B


Figure 10 Sensor location C

An existing finite element model of the bridge developed using *ANSYS* (ANSYS 2012) was used to extract the influence lines necessary for the fatigue analysis of the critical details. In the model, the deck and girders of the extension are modelled using SHELL182 elements, whereas the girders supporting the old bridge are modelled using BEAM188 elements.

The passing of a truck induces variable loading on the bridge. The repetitive loading and unloading of locations with high stress concentration, such as the welded joints of stiffeners, can provoke sudden failure of the given element for stress values well below the material's ultimate stress limit, due to crack formation and propagation. The fatigue resistance for a detail is given by its corresponding S-N curve, where the number of loading cycles for failure at a given stress range is plotted, usually in a logarithmic scale. Several tests were conducted (CECM/TC6 1987) in order to obtain normalized S-N curves for a wide variety of details. Results showed that the fatigue resistance S-N curve is linear with a slope of $m = 3$ when ploted in the log(S-N) plane and that it becomes horizontal at the threshold stress range for crack propagation $\Delta\sigma_D$, usually referred as the constant amplitude fatigue limit (CAFL). However, within the hypotheses of linear elastic fracture mechanics (LEFM), stress ranges below the CAFL can also contribute to fatigue damage, and therefore a modified S-N curve with a reduced slope of $m = 5$ under the CAFL can also be used, as suggested by EN 1993-1-9 (CEN 2003). SIA 263 (SIA 263 Code 2003b), on the other hand, gives the liberty of using an S-N curve with a single slope of $m = 3$ or $m = 5$. The resistance of a detail in terms of fatigue is thus categorized by the reference stress range value $\Delta\sigma_c$ (fatigue strength at 2×10^6 cycles) of its S-N curve, commonly abbreviated as the FAT category. The normalized fatigue resistance curves given by EN 1993-1-9 are presented in Figure 11.

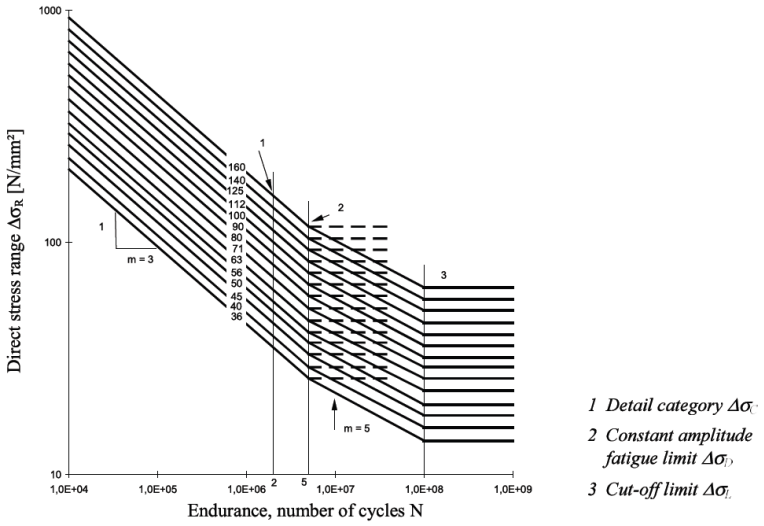

Figure 11 Normalized fatigue resistance curves (taken from EN 1993-1-9)

CD1 corresponds to a T-section stiffener located in the middle of the first span used to connect a transversal beam to the girders. The longitudinal welding, classified as FAT 56 according to SIA 263, that connects the stiffener to the bottom flange is considered for fatigue analysis. A fatigue reliability study of this detail was done by D 'angelo and Nussbaumer (2015), where results showed that the detail is safe with a reliability index of 9.14 for

a 100 year design life, assuming no increase in traffic. The critical detail and its FEM can be seen in Figure 11. The shape of the influence line for stress for the connection of this detail with the lower flange of the girder is presented in Figure 12.

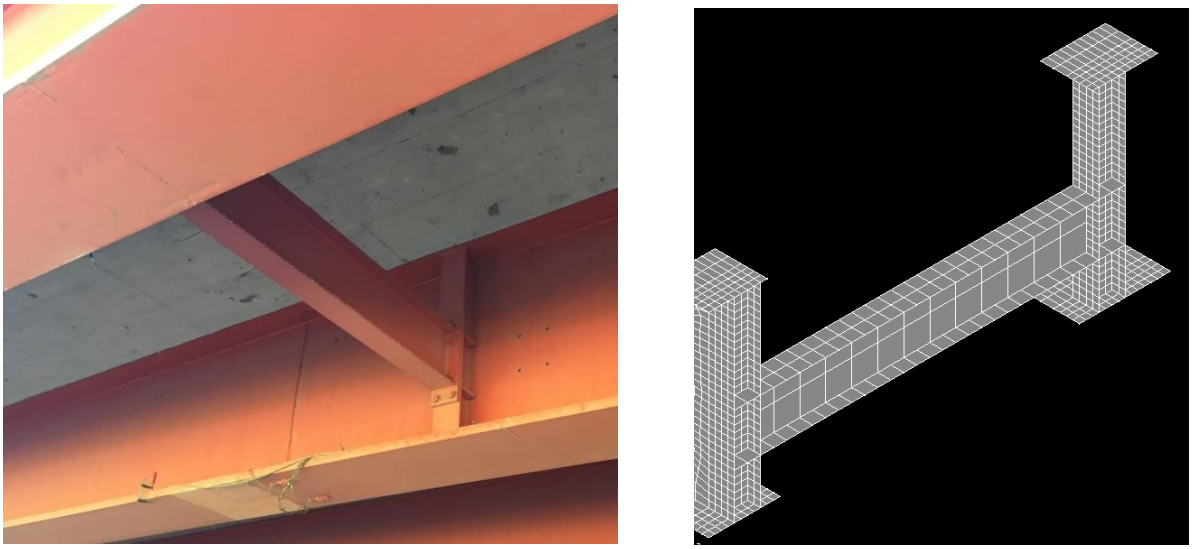

Figure 12 Location of critical detail 1 (left) and FEM of the detail (right)

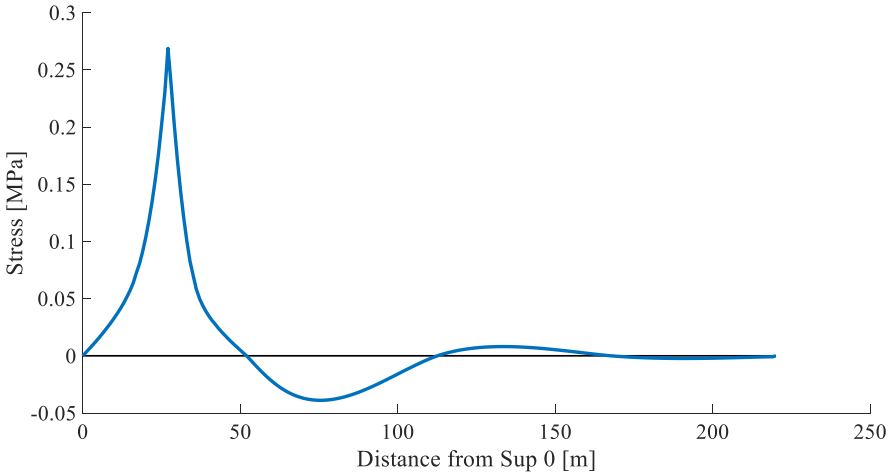

Figure 13 Representation of the shape of the influence line for CD1

The welded connection between a *200x55mm* stiffener and the upper flange of the girder at the second support, Sup 2 according to Figure 7, is considered for CD2. This type of detail is categorized as FAT 56 according to SIA 263. In Figure 13 the critical detail and its FEM is presented. The shape of the influence line for stress for the connection between CD2 and the girder's upper flange is shown in Figure 14.

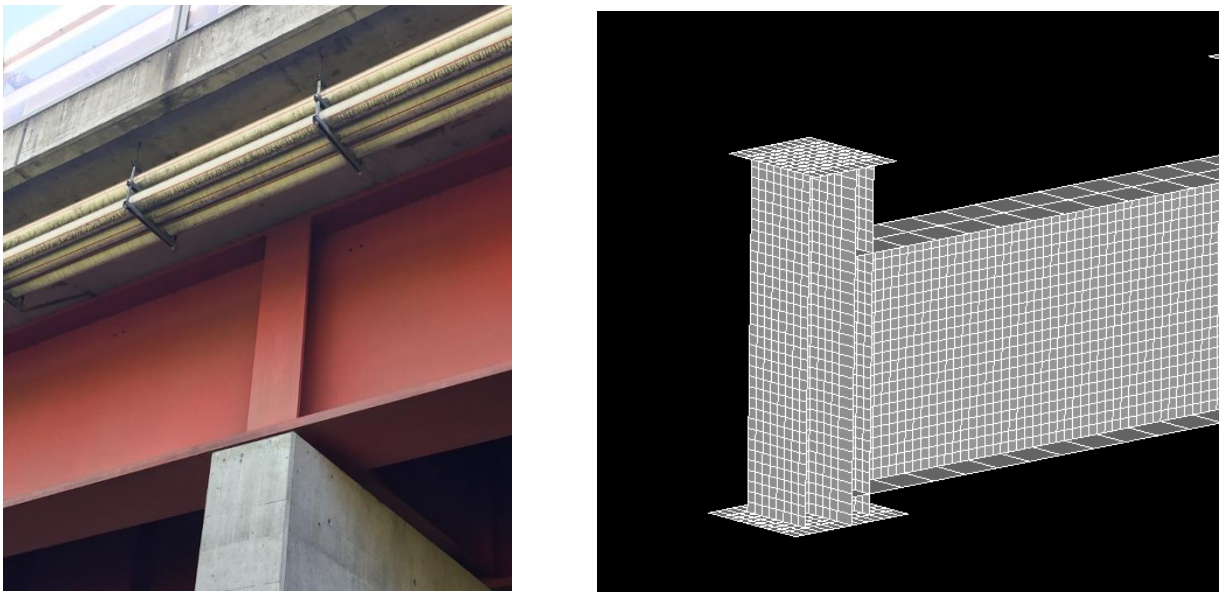

Figure 14 Location of critical detail 2 (left) and FEM of the detail (right)

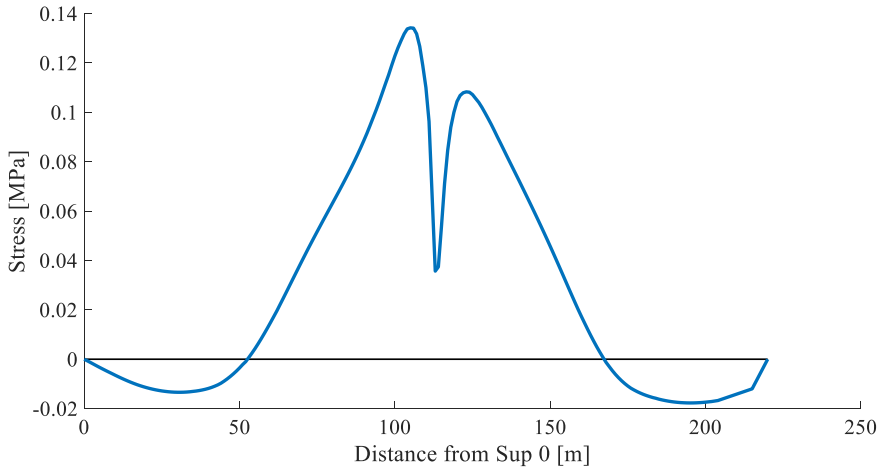

Figure 15 Representation of the shape of the influence line for CD2

The stiffener considered as CD3 is the similar to CD1, as can be seen in Figure 15, but located in the middle of the third span. Therefore, the fatigue classification according to SIA 263 is also FAT 56 for this case. The shape of the influence line for stress for the welded connection between CD3 and the bottom flange of the girder is presented in Figure 16.

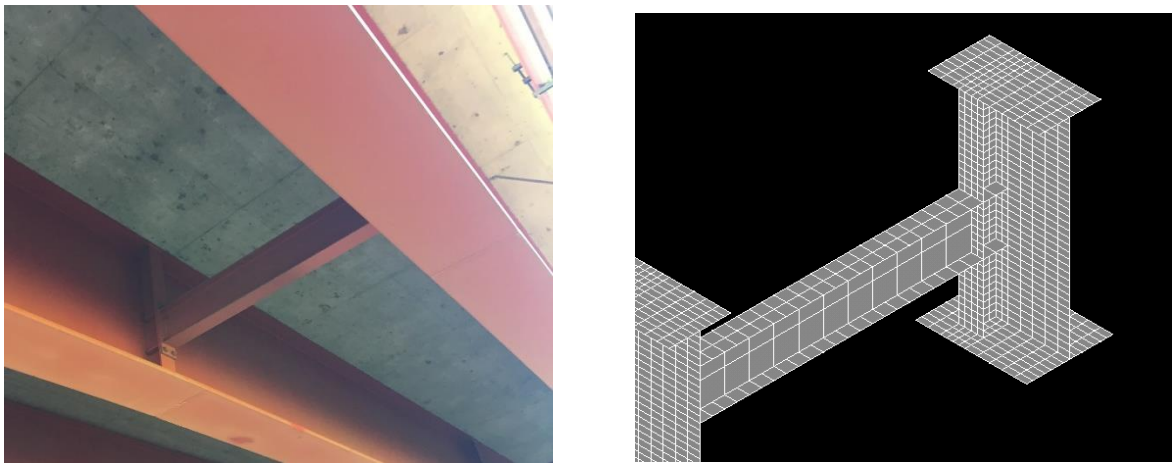

Figure 16 Location of critical detail 3 (left) and FEM of the detail (right)

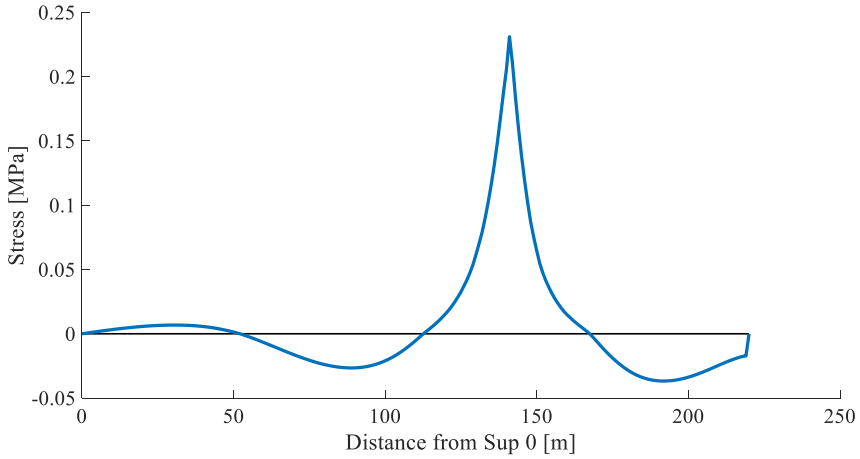

Figure 17 Representation of the shape of the influence line for CD3

4.2 Sensor and traffic load data

Reserve fatigue life can be estimated using the in-service data provided by the strain gauges. Strain measurements recorded by sensors B1, B2, B3 and B4 from 18/11/2013 to 24/11/2013 are used to update knowledge regarding the behavior of the bridge. A time history of strains is obtained from measurements, which needs to be converted into a physical quantity that enables data-interpretation.

Having a stress time distribution, obtained by multiplying the strain time history by the Young's modulus of steel, the stress histogram for a given sensor location is computed using the rainflow algorithm (Downing and Socie 1982). Stress values below 2 MPa are not considered in the analysis given their low contribution to fatigue damage. The stress time history for sensor B1 and its corresponding stress histogram are presented in Figures 17 and 18, respectively. The stress time history and histograms for the all sensor locations can be found in Appendix B and C.

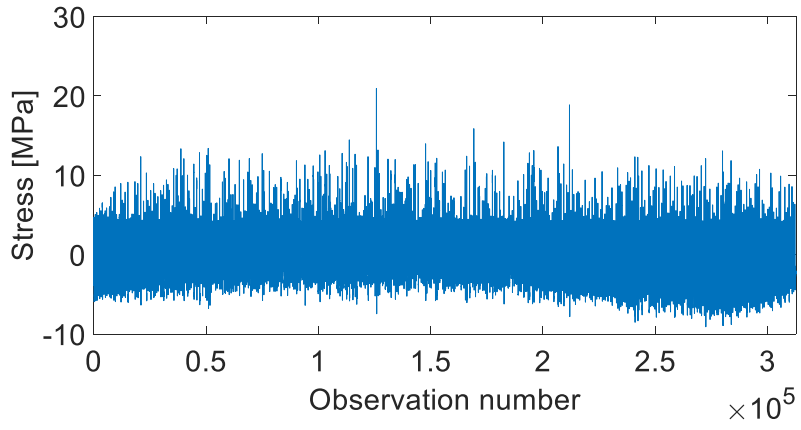

Figure 18 Stress time history for sensor B1

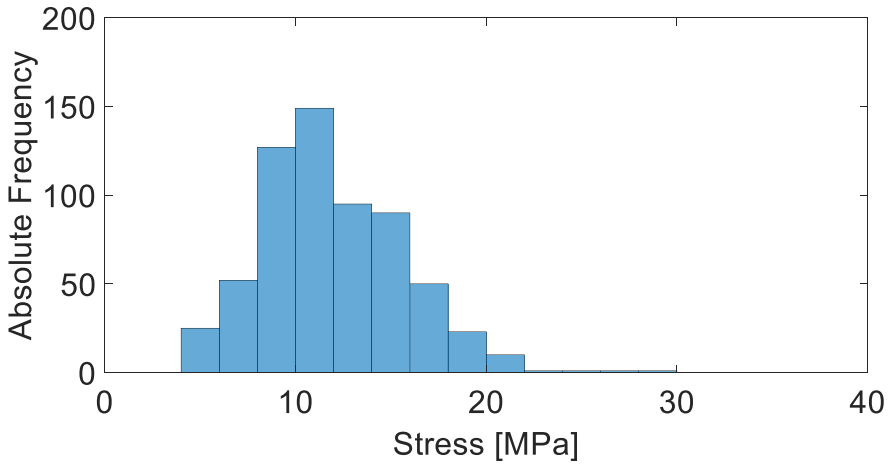

Figure 19 Stress histogram for sensor B1

Having obtained the stress histogram for each location, the fatigue damage corresponding to the period considered is given by Miner's rule (Miner 1945) :

$$D = \sum \frac{n_i}{C \cdot \Delta\sigma_i^{-m}} \tag{15}$$

In Eq. 15 n_i corresponds to the number of cycles for a given stress range $\Delta\sigma_i$, m to the slope of the S-N curve considered and C a constant that depends on the critical detail. Sensor data needs to be translated into a quantity that is comparable to model predictions. Therefore, an S-N curve with m=3 and C constant with respect to a FAT56 critical detail are adopted, given that all critical details studied belong to this category. Finally, since one week of sensor data is considered, remaining fatigue life is calculated by :

$$RFL = \frac{1}{52 \cdot D_{week}} \tag{16}$$

As for model predictions, traffic information gathered from a weigh-in-motion (WIM) station is used alongside the finite element model of the bridge to compute remaining fatigue life for each model instance. A WIM station,

located 1km away from the bridge, provides data regarding heavy traffic load, more specifically time of passage, speed, number of axles, total length, gross total weight, axles weight and distance between axles of trucks that passed in the considered period. Having this information, an axle train is generated and passed over the influence line for stress, for each desired location. Consequently, a stress time history is obtained and remaining fatigue life can be calculated by following the aforementioned procedure. The shape of the influence line for sensor B1 is shown in Figure 19. The shape of the influence lines for all locations considered can be found in Appendix D.

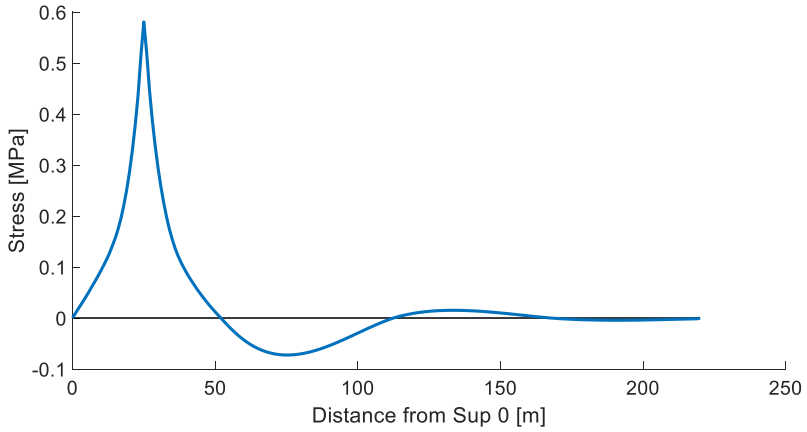

Figure 20 Representation of the shape of the influence line for sensor B1

4.3 Model class

Identifying every parameter that has an influence on structural response is an unfeasible task. Therefore, a sensitivity analysis was conducted in order to determine the parameters that most influence the response of the bridge.

Parameter	**Abbreviation**	**Units**	**Range**
Elastic modulus of steel	Es	GPa	190 - 210
Elastic modulus of concrete	Ec	GPa	20 - 40
Connection between concrete deck and steel girders longitudinally	KDECKX	log N/mm	4 - 6.5
Connection between concrete deck and steel girders transversally	KDECKZ	log N/mm	4 - 7
Vertical stiffness of Sup 0	KYO	log N/mm	3 - 6.5
Horizontal stiffness of Sup 0	KXO	log N/mm	3 - 7
Rotational stiffness of Sup 0	ROTZO	log Nmm/rad	9 - 14
Vertical stiffness of Sup 1	KY1	log N/mm	5.5 - 8
Horizontal stiffness of Sup 1	KX1	log N/mm	2 - 5

Table 4 Initial range adopted for the parameters that influence structural response

Engineering judgment is used to first define initial beliefs regarding parameters that affect structural response at sensor locations. These parameters and the initial range of values considered for them are presented in Table 4. In order to study the response of the bridge to the variation of these parameters, a linear regression of the structure's response was computed using Box-Behnken design (Box and Behnken 1960), for each measurement location.

$$R = \beta_1\theta_1 + \beta_2\theta_2 + \cdots + \beta_k\theta_k \tag{17}$$

In Eq. 17 structural response R is expressed as a linear combination of the structure's parameters θ_k. The regression coefficients β_k can be interpreted as weights that indicate the relative importance of a given parameter in structural response. Two analyses were carried out, with respect to the most critical loading cases for the sensor locations – when the traffic load is located in the middle of the first span and when it is located on top of the first support. The mean values between both cases are considered for model class selection.

Parameter	**Relative importance (%)**	
	Sensor B	**Sensor C**
Es	2.12	3.57
Ec	14.22	7.28
KDECKX	42.44	44.76
KDECKZ	15.6	17.03
KYO	3.15	0.08
KXO	1.49	0.76
ROTZO	1.62	4.56
KX1	3.99	0.98
KY1	15.36	20.99

Table 5 Relative importance of the parameters on structural response

Scrutinizing Table 5 it can be observed that the parameters that have the most influence on structural response are Ec, KDECKX, KDECKZ and KY1. Therefore, these are the parameters adopted to constitute the model class for updating knowledge regarding structural behavior.

4.4 Surrogate modelling

Several model instances, i.e. combinations of model class and parameter set, are generated in order to carry out system identification. Each model instance corresponds to a different set of parameter values and therefore a different influence line that has to be extracted from the FE model of the bridge. Doing so for every model instance generated is computationally expensive, thus surrogate models have to be developed to overcome large simulation times. A latin hypercube sample (McKay et al. 1979) of three hundred model instances is generated and influence lines for the locations of the sensors and critical details are extracted from the FE model, for each model instance. RFL is calculated for these influence lines and used to train neural network models that make a

regression of this data. A neural network is built for each location and used to make RFL predictions. For validation, on the other hand, neural networks are used to predict equivalent stress range for sensors C1 and C2. Equivalent stress range $\Delta\sigma_e$ (Bannantine et al. 1990) for a given influence line is computed in an analogous manner as described in section 4.2, using Eq. 18 :

$$\Delta\sigma_e = \left(\sum \frac{n_i \Delta\sigma_i^m}{\sum n_i}\right)^{\frac{1}{m}} \tag{18}$$

where n_i is the number of cycles for a given stress range $\Delta\sigma_i$ and m the slope of the S-N curve. A more detailed decription of the surrogate modelling methodology is presented in Appendix E.

4.5 Sources of uncertainty

Several sources of uncertainty other than measurement error have to be accounted for in order to make correct data-interpretation. Most of these sources cannot be parameterised and can only be estimated using engineering heuristics. In this section, a description of the methods used to estimate the principal sources of modeling uncertainty is presented.

4.5.1 Secondary parameter uncertainty

Making assumptions regarding parameters that are not included in the model class induces errors in model predictions. These errors contribute to secondary parameter uncertainty. To estimate this uncertainty, structural response was computed for a Box-Behnken design of the secondary parameters and compared to the structural response obtained when considering the mean value of the ranges presented in Table 4.

$$\varepsilon_{secondary} = \frac{g_i(\theta^*) - g_i(\theta)}{g_i(\theta^*)} \tag{19}$$

In Eq. 19 $g_i(\theta^*)$ corresponds to the structure response at a given location computed with the mean value of the parameters, and $g_i(\theta)$ the response computed with a certain combination of secondary parameters given by the Box-Behnken design. When adopting this procedure, stress values at each sensor location vary between -1.2% and 2.2% of the stress obtained when taking the mean value for the parameters, i.e. $g_i(\theta^*)$. Therefore, based on the principle of maximum entropy (Jaynes 2003), secondary parameter error is considered to have a uniform distribution between -1.2% and 2.2%.

$$U_{secondary} \sim U(-1.2\%\,,\ 2.2\%)$$

4.5.2 Surrogate model error

As described in section 4.4, neural networks are used to make predictions regarding RFL and equivalent stress range for several locations. Neural networks make a regression of the input data set, allowing predictions to be made. Naturally, errors arise when regressions are made. A perfect fit to the data is unattainable. To estimate

surrogate modeling error, a comparison has to be made between predictions obtained with the surrogate models and structural response extracted from the FE model of the bridge. To achieve that, preliminary surrogate models were developed, using 250 of the 300 samples mentioned in section 4.4. RFL corresponding to the remaining 50 model instances were predicted using the preliminary neural networks and compared to the values obtained when following the procedure presented in 3.2.

$$\varepsilon_{surr.\ model} = \frac{g_i(\theta^*) - g_i(\theta)}{g_i(\theta^*)} \tag{20}$$

In Eq. 20 $g_i(\theta^*)$ now represents RFL computed with an influence line extracted from the FE model corresponding to a given model instance, and $g_i(\theta)$ the RFL prediction for that model instance when using the preliminary surrogate model developed. Errors at sensor locations vary between -20% and 15%, and therefore surrogate model error is considered to have a uniform distribution between these values.

$$U_{surr.\ model} \sim U(-20\%\,,\ 15\%)$$

4.5.3 Model bias

Simplifications and omissions are inherent to the modeling process of civil engineering structures. To reduce computational time, simplifications were made to the influence lines extracted from the FE model. Stress values were obtained while passing the load over a reduced number of points along the bridge, which resulted in poorly discretized influence lines, as depicted by Figure 20.

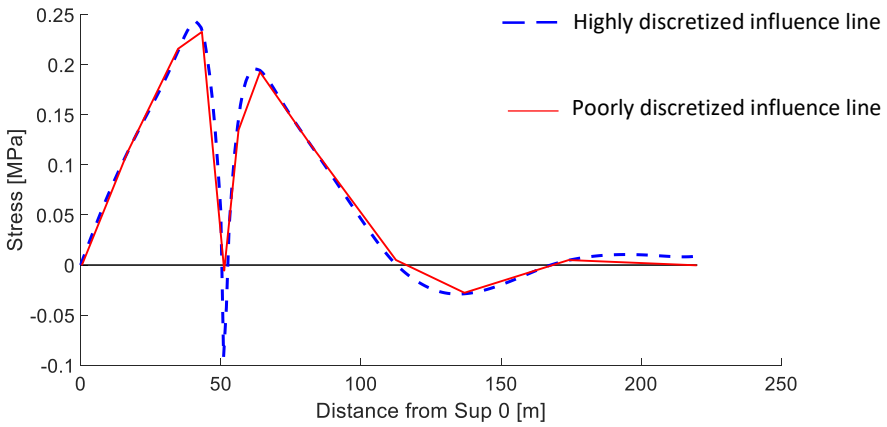

Figure 21 Simplified influence line for sensor C1

RFL was calculated for all sensor locations using both a highly discretized influence line and a poorly discretized influence line, obtained with the mean parameter values. The highest difference in results observed was equal to 9.22%. There are many other sources of uncertainty that lead to model bias such as not considering cracking in the concrete deck, mesh density considered in the FE analysis, non-linear behavior of materials, etc. In addi-

tion, quantifying the uncertainty related to these sources is difficult. Engineering judgment is thus used to estimate their effect on structural response. Consequently, uncertainty related to model bias is assumed to be described by a uniform distribution between -2% and 10%.

$$U_{model\ bias} \sim U(-2\%\ ,\ 10\%)$$

4.5.4 Other sources of uncertainty

Other sources of uncertainty have influence on the structural behavior such as the position of the traffic load on the bridge, uncertainty related to the data gathered from the WIM station, measurement error. The distributions for these sources were determined based on previous experience (Pai et al. (2017); Pasquier et al. 2014, 2016). A summary of the sources of uncertainty considered is presented in Table 6.

Source	Distribution	Min/Mean	Max/Std. dev.
Secondary parameters (%)	Uniform	-1.2	2.2
Surrogate model (%)	Uniform	-20	15
Model bias (%)	Uniform	-2	10
Traffic load (%)	Uniform	1	3
Vehicle position (%)	Uniform	0	3
Measurement error (%)	Gaussian	0	0.5

Table 6 Sources of uncertainty

These ucertainties are combined using Monte Carlo simulation in order to obtain the combined uncertainty PDF based on which the threshold bounds for EDMF are computed and the likelihood function is constructed for BMU. The combined uncertainty PDF for the sources of uncertainty presented in Table 6 is shown in Figure 21. It can be noted that the PDF is biased from zero and does not follow a Gaussian distribution.

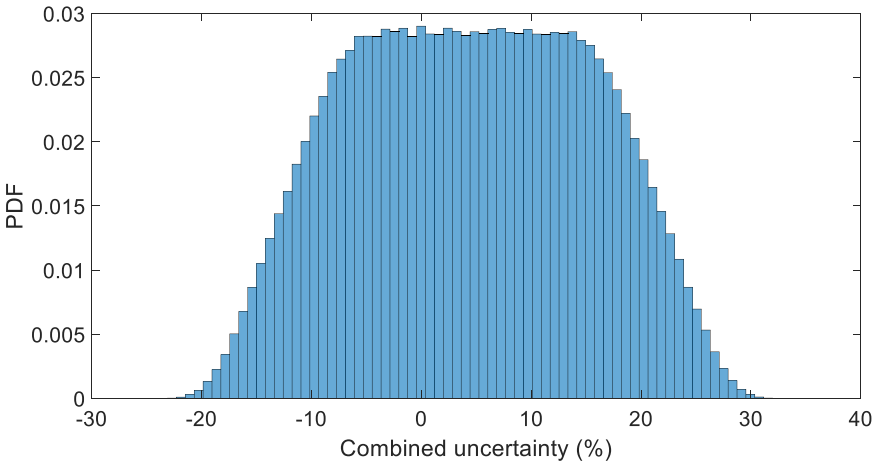

Figure 22 Combined uncertainty PDF

4.6 Structural identification

Identification results using residual minimization, BMU and EDMF are presented in this section. For EDMF, threshold bounds were computed for a target reliability $\phi = 0.95$ and 88469 models were falsified out of 100000 model instances generated. For BMU, the ranges presented in Table 4 define uniform distributions that are updated with a likelihood function based on the combined uncertainty PDF. Uncertainties at various measurement locations are assumed to be independent, therefore the covariance matrix Σ assumes the form of a diagonal matrix, where all the non-zero elements are equal to the variance of the combined uncertainty PDF. One million samples using Markov Chain Monte Carlo simulation are used to obtain the posterior distribution, with verified convergence. As for residual minimization, one single solution is found, corresponding to the model instance with the smallest weighed sum of the square of the residuals over every measurement location. Fatigue life predictions using the three methodolgies for the sensor locations used for updating are plotted in Figue 22.

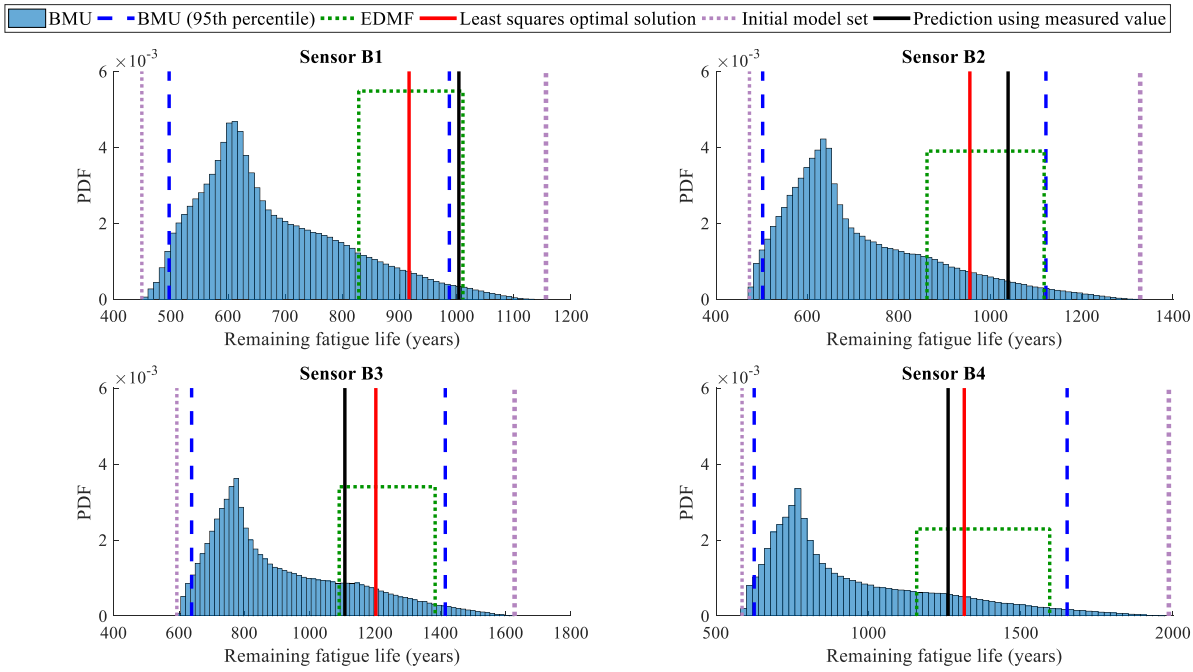

Figure 23 Identification using information obtained from sensors B1, B2, B3 and B4

The first observation that can be asserted, when analyzing Figure 22, is the large bias between the posterior distribution obtained with BMU and the value for RFL computed when using measured values. Taking results from sensor B1 as means of comparison, RFL prediction using the initial parameter set varies between 449 and 1157 years whereas the 95th percentile of the posterior distribution obtained with BMU contains predictions that vary between 495 and 987 years. Moreover, the 95th percentile of the posterior obtained for sensor B1 does not include the value obtained using measurements. The reduction in uncertainty after updating knowledge with BMU is not significant. EDMF, on the other hand, provides robust identification with reduction in uncertainty. RFL predicted using the candidate models filtered by EDMF lies between 829 and 1011 years for sensor B1. The bounds given by EDMF for RFL prediction include the value obtained from measurements in all locations considered. Results obtained from residual minimization are inconsistent. For sensors B1 and B2, these results give an

underestimation of RFL when compared to the value computed using measurements, while overestimated predictions are obtained for sensors B3 and B4.

Identification results are presented in Figures 23 and 24, where the posterior distributions obtained through BMU for each parameter of the model class are plotted in the former, and a parallel axis plot of the candidate models filtered through EDMF is shown in the latter.

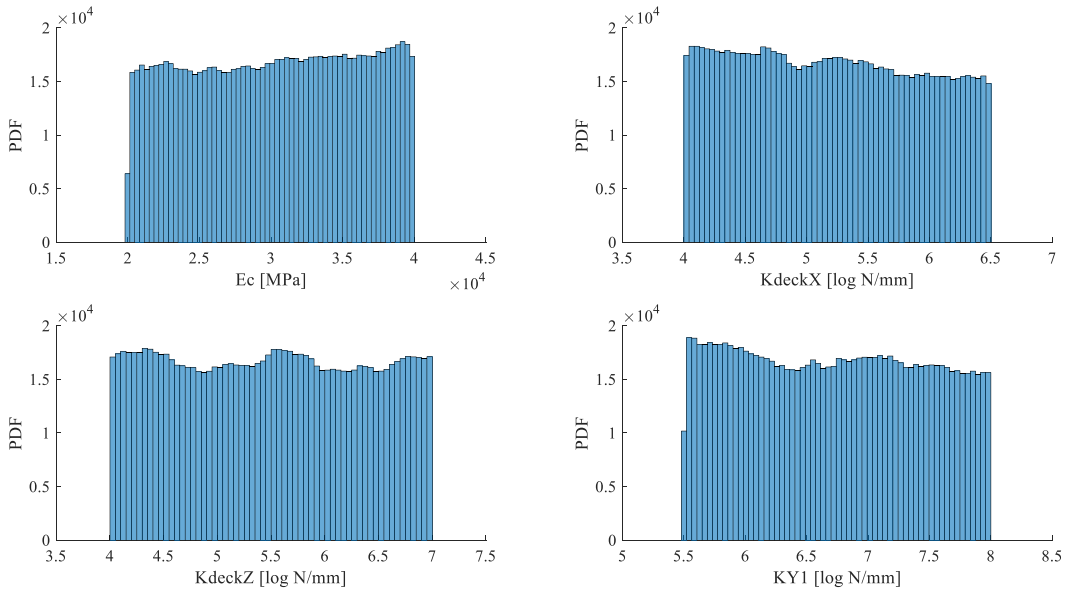

Figure 24 Identification of parameters using BMU

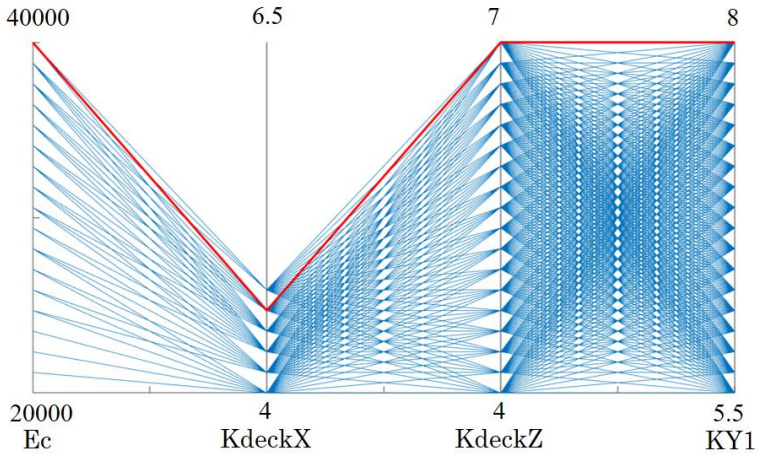

Figure 25 Parallel axis plot of candidate models using EDMF (blue) and optimal solution using residual minimization (red)

The same remark can be made when analyzing Figures 23 and 24. Uniform posterior distributions are obtained from BMU for the parameters that are being identified, meaning that there was no reduction in uncertainty after updating the models with measurements. In Figure 24 a parallel axis plot of the candidate models identified using EDMF is presented. The initial range of values for each parameter is divided into 18 instances, as a result of grid sampling. Each candidate model is represented by a line that intercepts each axis on the parameter values of the accepted model instance. On the contrary, the lack of a line connecting parameter values indicates a falsified

model. For instance, the values 40000, 6.5, 7 and 8 are not connected, which means that the response for the model instance corresponding to this combination of parameter values does not lie within the defined threshold bounds, hence the model instance is falsified. A reduction in uncertainty related to the parameter KdeckX can be seen, when inspecting Figure 24. The initial range of values defined for this parameter – [4 6.5] – is reduced to [4 4.7353] as a result of applying the EDMF methodology. The optimal model instance identified using residual minimization is included in the candidate models given by EDMF. This can be observed in Figure 24, where the line that depicts the solution obtained with residual minimization is coincident with a line that represents the same model instance accepted by EDMF. Similarly, it can be seen on Figure 22 that RFL prediction bounds given by EDMF incorporate the prediction of the least squares optimal solution for all measurement locations.

4.7 Validation

Knowledge regarding structural behavior was updated using three different data-interpretation techniques. In order to validate results, updated knowledge is used to predict equivalent stress range at two different locations – sensors C1 and C2. Predictions for equivalent stress range obtained with the three methodologies for these locations are shown in Figure 25.

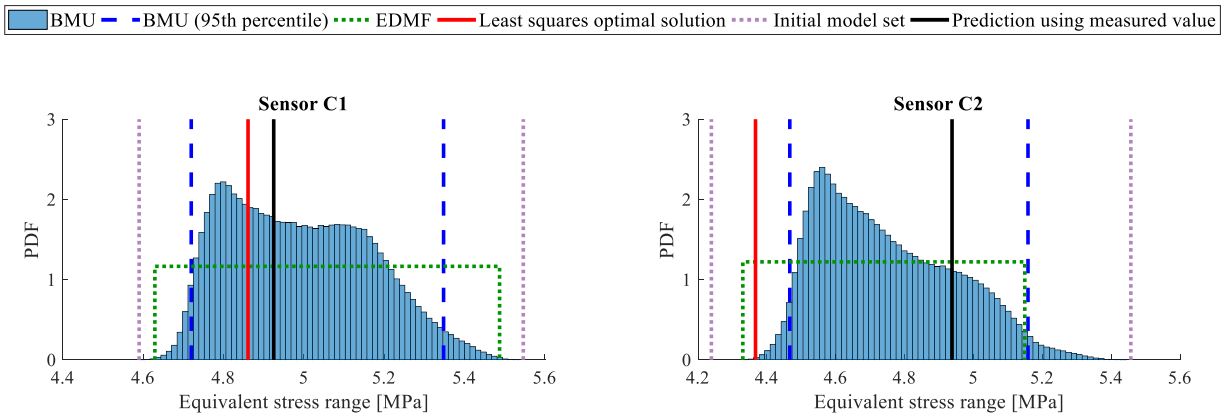

Figure 26 Equivalent stress range predictions for sensors C1 and C2

Using the equivalent stress range computed with the measured value as reference, it can be seen in Figure 25 that EDMF provides with a wide yet robust prediction of equivalent stress range. For sensor C1, the value obtained using measurements is equal to 4.9 MPa and predictions obtained with EDMF vary from 4.6 MPa to 5.5 MPa. As for sensor C2, equivalent stress range predicted using EDMF lies between 4.3 Mpa and 5.1 MPa, whereas the value computed using measurements is 4.9 MPa. The maximum likelihood estimate (MLE) of the posterior distribution obtained from BMU is equal to 4.8 MPa for sensor C1 and 4.55 MPa for sensor C2. A larger bias of the MLE of the predicted distribution resulting from BMU is obtained for sensor C2, when compared to the values computed with measurements. Moreover, while a conservative bias is obtained for RFL prediction, BMU gives an underestimation of equivalent stress range for sensors C1 and C2, i.e. non-conservative predictions. The same remark can be made to equivalent stress range predictions obtained with residual minimization. The optimal set of parameters gives a prediction of 4.86 MPa for sensor C1 and 4.4 MPa for sensor C2.

4.8 Remaining fatigue life prediction for the critical details

Having updated knowledge regarding the structure's parameters, remaining fatigue life predictions can be made for unmeasured locations. Three different details were considered, as described in section 4.1. RFL for the bridge is dictated by critical detail 1, as it is the detail with lowest fatigue life. Fatigue life computed for this detail with the initial set of parameters is 474 years. EDMF predicts a RFL for this location that varies from 863 to 1124 years. The MLE of the posterior distribution obtained with BMU is 635 years. Prediction using the optimal solution retrieved with residual minimization gives a RFL of 957 years. Fatigue life prediction for the other critical details are presented in Table 7.

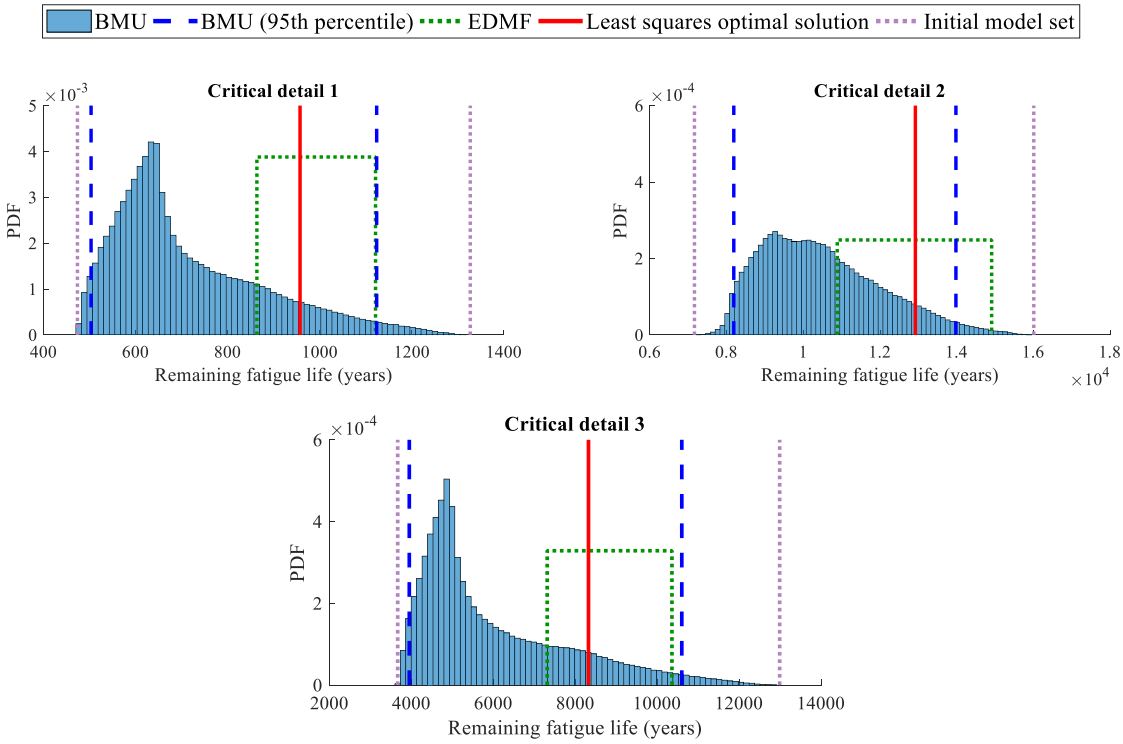

Figure 27 Fatigue life prediction for different critical details

	Remaining fatigue life (years)			
	EDMF		BMU (MLE)	Residual minimization
	Lower bound	Higher bound		
CD1	863	1124	635	957
CD2	10880	14910	9263	12920
CD3	7317	10360	4864	8325

Table 7 RFL predictions for three different critical details

5. Robustness of the data-interpretation methodologies

Data-interpretation methodologies can be extremely useful when design-model predictions show that the remaining fatigue life of a structure is below its required service life (Pasquier et al. 2016). A more thorough fatigue assessment can be made and the reduction in uncertainty resulting from employing model-based data interpretation may show that the structure possesses reserve capacity, which prevents unnecessary repair or retrofit. Therefore, decision-making is dependent on results obtained from data-interpretation. To assist and enable better decision-making, data-interpretation techniques have to be accurate, easy to employ and understand, and robust to variations in uncertainty. As stated before, uncertainties related to civil engineering structures are hard to quantify. These uncertainties can be estimated based on engineering judgment, as was done in section 4.5, but ultimately they can have different values than the ones presented in Table 7.

A graphical user interface (GUI) toolbox was developed to assist in decision-making, where different scenarios related to uncertainty estimation can be considered. The source code for this toolbox can be found in Appendix F. Results from the three data-interpretation techniques are shown through a plot of remaining fatigue life prediction for sensor B1. With this toolbox, the user can study the robustness of EDMF, BMU and residual minimization to variations in uncertainty and make decisions based on differences observed and the level of risk desired. In the toolbox, the sources of uncertainty that are harder to estimate – model bias, vehicle position and surrogate model error – can be varied according to three different scenarios – low, medium and high uncertainty. For the model bias, a variation of 5% to the upper bound of the PDF is introduced when choosing a given scenario, reflecting the user's belief regarding the conservativeness of the model. Vehicle position uncertainty is related to errors introduced by not considering small variations that can occur in the trajectory of a passing truck. A variation of 2% in uncertainty between different scenarios is considered to account for the difficulty in estimating this effect. As mentioned in section 4.5.2, preliminary surrogate models trained with 250 samples of model instances are used to estimate surrogate modeling error. Albeit giving us an approximation of the error, the entirety of the 300 samples are used to train the neural networks that are used for prediction, and therefore the true value for the error related to surrogate modeling can't be determined. For this reason, a variation of 10% corresponding to a 5% change in both the lower and upper bound of the surrogate model error is made when adopting different scenarios in the toolbox.

	Uncertainty scenario		
	Low	Medium	High
Model bias	[-2% 5%]	[-2% 10%]	[-2% 15%]
Vehicle position	[0% 1%]	[0% 3%]	[0% 5%]
Surrogate model error	[-15% 10%]	[-20% 15%]	[-25% 20%]

Table 8 Uncertainty scenarios considered in the toolbox

The toolbox is composed by two different tabs, one where the changes to the combined uncertainty PDF due to the choice of different scenarios can be observed, and another where identification results obtained with the three methodologies considered are shown, for sensor B1. The first tab is displayed on Figures 27 and 28.

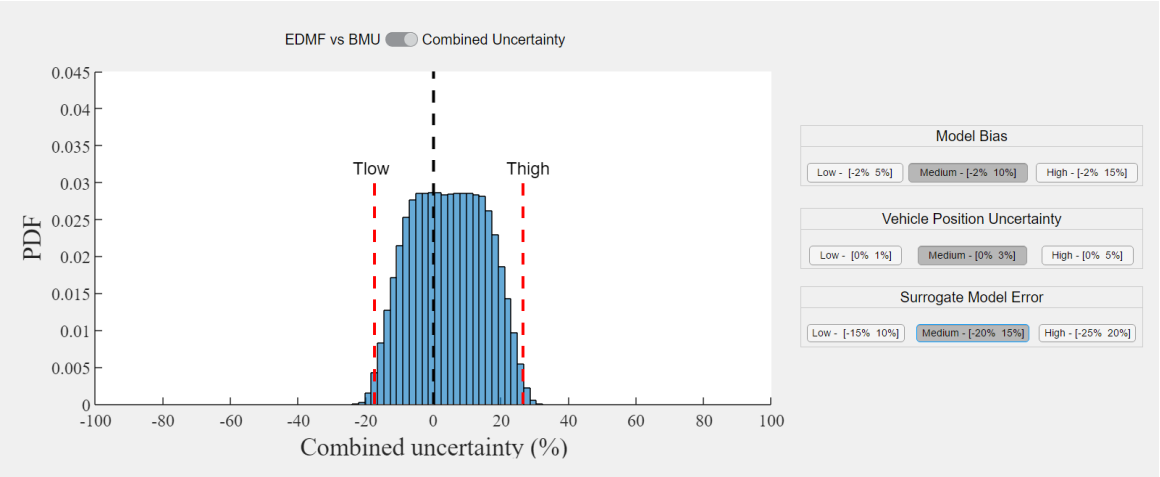

Figure 28 Combined uncertainty PDF displayed on the toolbox for the scenario considered in section 4.5

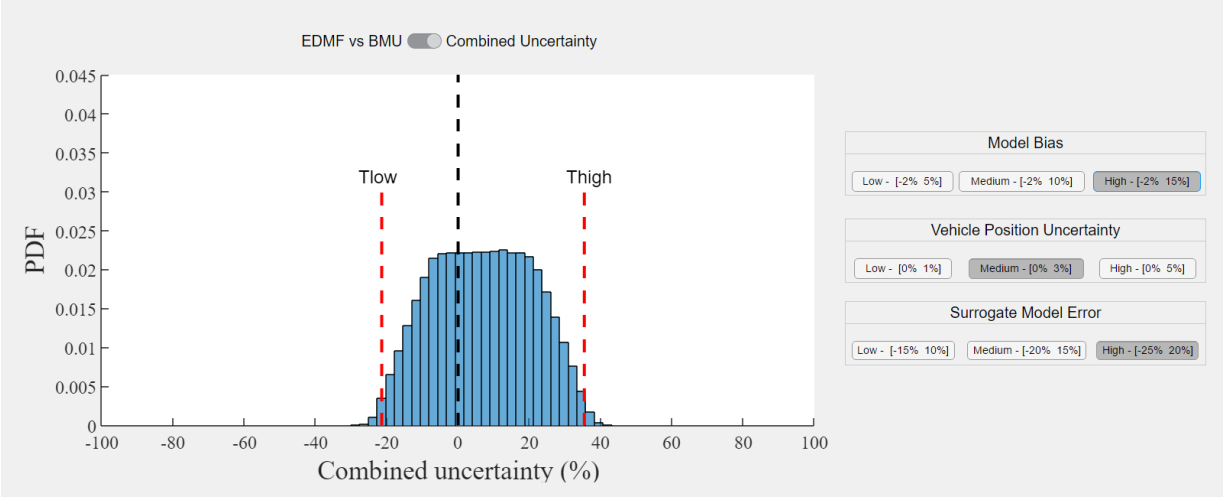

Figure 29 Combined uncertainty PDF for a scenario with high model bias and high surrogate model error

Thresholds bounds used for falsification in the EDMF methodology are also shown in this tab, as shown in Figures 27 and 28. It can be seen that, for different uncertainty scenarios considered, the combined uncertainty PDF is not centered on zero.

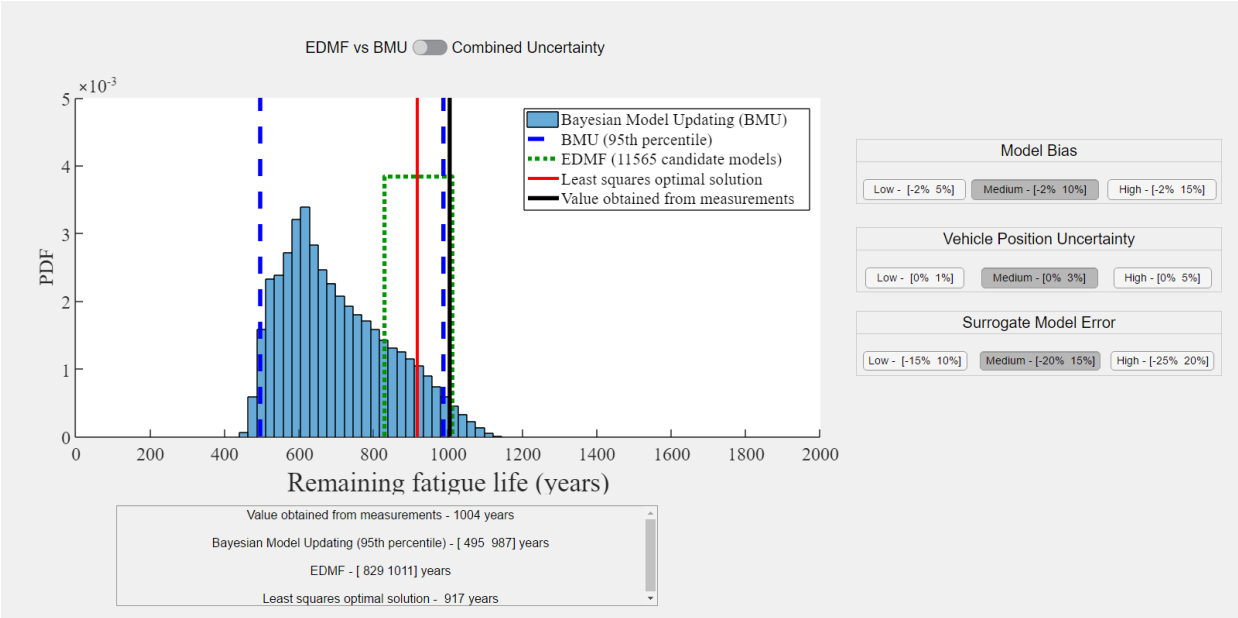

Figure 30 Data-interpretation results for sensor B1 for a scenario of medium uncertainty for all sources

The second tab is presented in Figure 29, where identification results for sensor B1 are shown. The default configuration for the uncertainties is set to medium. Consequently, the results shown are the same as presented in section 4.6. This toolbox permits the user to express beliefs regarding the modeling process and make decisions based on observed results. Ultimately, it is the decision-maker's responsibility to choose the scenario deemed to fit best, but there are certain combinations of uncertainty that are worth considering, where the difference in fragility to misevaluated uncertainty can be observed for the different data-interpretation techniques. The low uncertainty scenario for model bias is one of these cases. In section 4.5.3 it was shown that simplifications made to extracted influence lines can introduce a 10% error in model predictions. Therefore, taking a 5% higher bound for model bias is a clear misevaluation of this source of uncertainty. RFL predictions for this scenario – low model bias – using the GUI toolbox is shown in Figure 30.

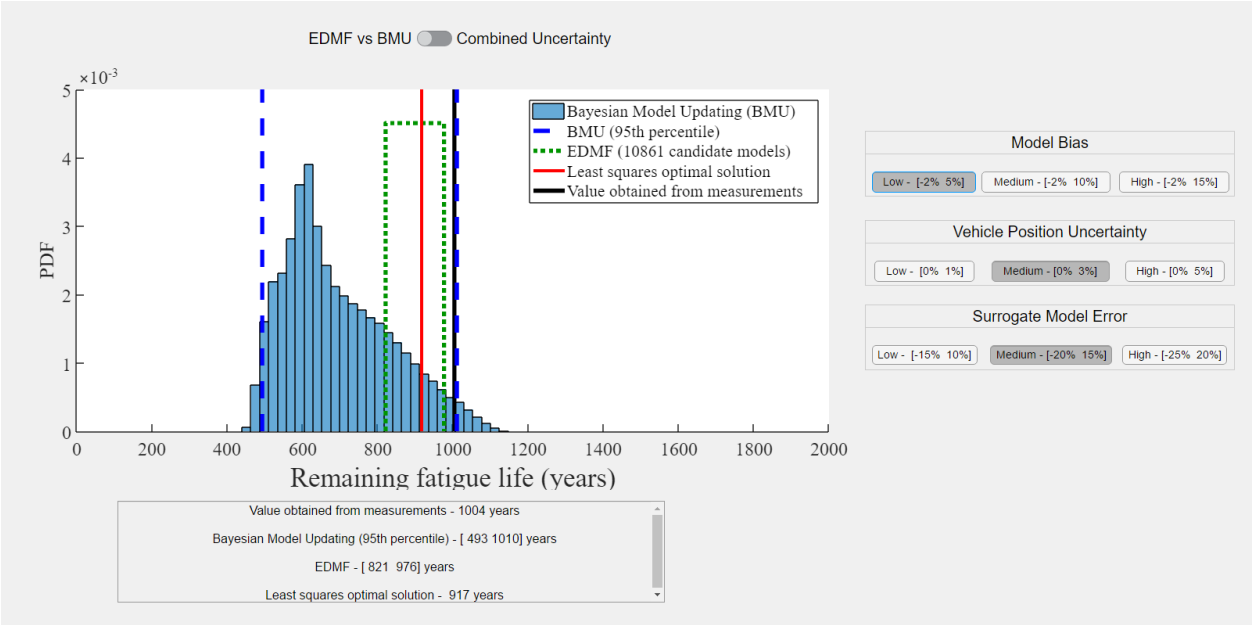

Figure 31 Low uncertainty scenario for model bias

As shown in Figure 30, EDMF results for this scenario do not include the value obtained from measurements, and therefore suggests that a review on initial assumptions and quantification of uncertainties is needed. The residual minimization technique calibrates parameters in order to find one single solution that minimizes the squared sum of residuals. This procedure does not take modeling errors into account and therefore it is not sensible to the variation of uncertainty. Goulet and Smith (2013) have shown the drawbacks and limitations of utilizing this technique. A wrong estimation of model bias does not have much effect in results given by BMU. In fact, the 95th percentile of the posterior distribution given by BMU changes from not including the value obtained from measurements to including it, when changing scenarios from medium to low model bias. This would wrongly induce the user to think that the low uncertainty scenario is a correct estimation for model bias. Additionaly, when it comes to decision-making, the conservative, i.e. lower bound is usually taken as a reference. The lower bound for the 95th percentile changes from 495, for the medium scenario, to 493 years when considering low model bias. A negligible change occurs in results given by BMU when wrongly estimating model bias. Only results given by EDMF give suggestions regarding the correct estimation of model bias. Presented with this circumstance, the user should be inclined to choose high uncertainty for model bias, providing that a higher bound of 10% only accounts for the simplification made regarding influence lines, and several other sources of uncertainty in the modeling process contribute to model bias.

Regarding vehicle position uncertainty, the toolbox can be used to verify that changes in this source of uncertainty do not have much effect on results for any of the methodologies. This can be observed in Figures 31 and 32.

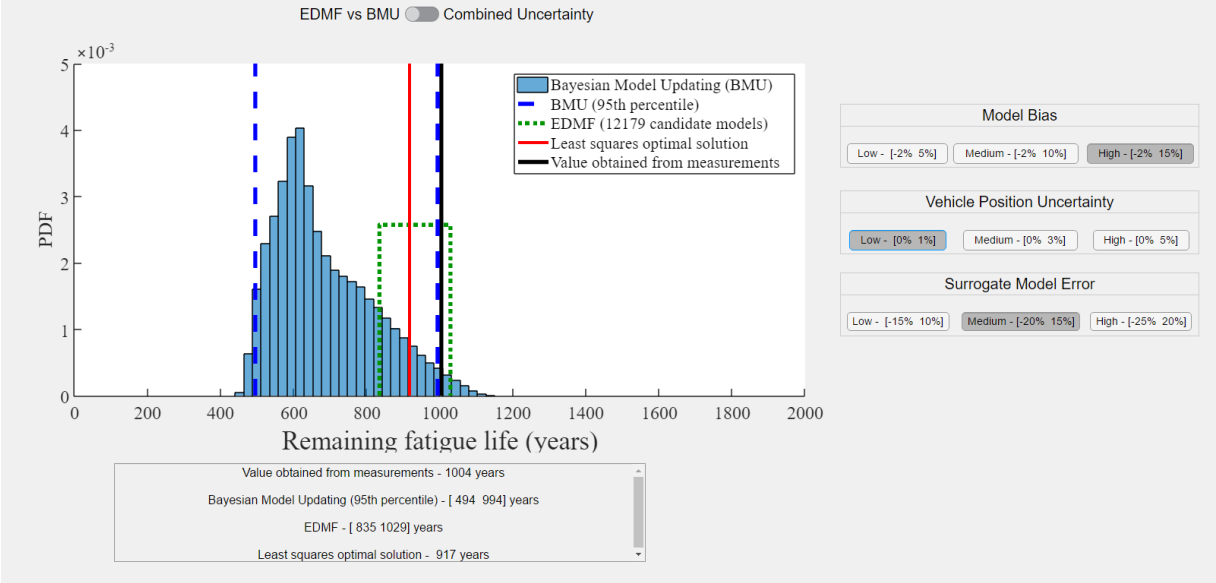

Figure 32 Low vehicle position uncertainty scenario

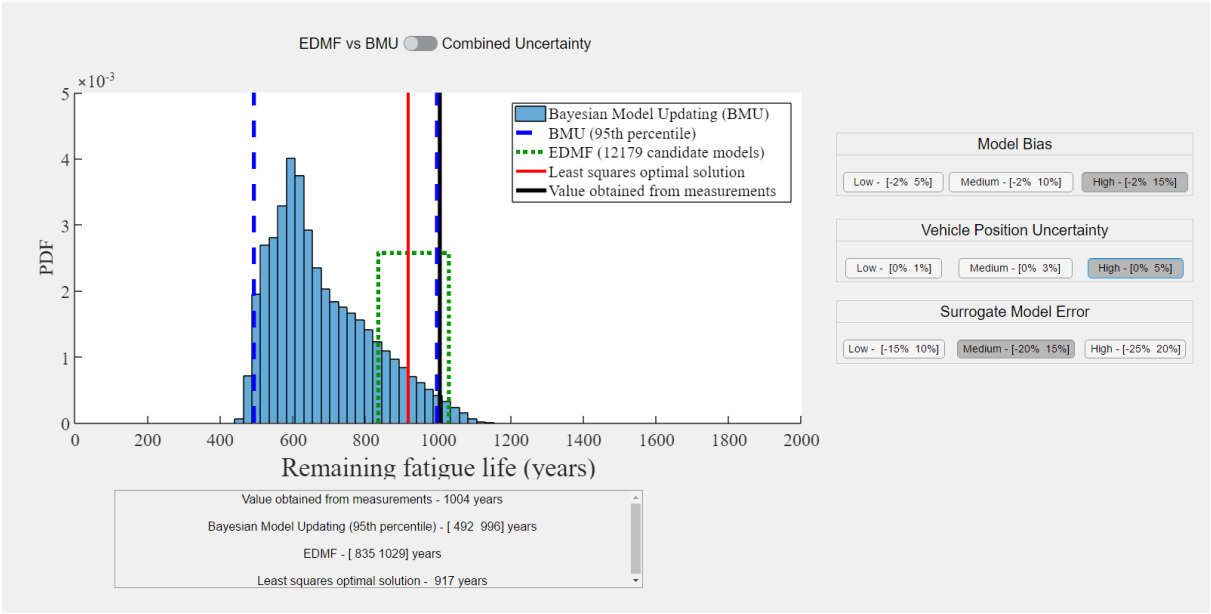

Figure 33 High vehicle position uncertainty scenario

Beliefs regarding the optimality of the regression made by the neural networks is expressed when choosing different levels of uncertainty for surrogate model error. When considering different scenarios for this error, results obtained with BMU do not suffer much change. In Figures 33, 34 and 35 RFL predictions for sensor B1 are shown, when considering low, medium and high surrogate model error, respectively. The lower bound for the 95th percentile of the posterior distribution gives RFL predictions of 492 years for medium and high uncertainty, and 499 years for low uncertainty scenario. Similarly to when model bias was varied, changes in predicitons obtained with BMU resulting from varying surrogate modeling error are also negligible. The lower bound given by EDMF changes from 879, 834 and 789 when considering the low, medium and high scenarios, respectively.

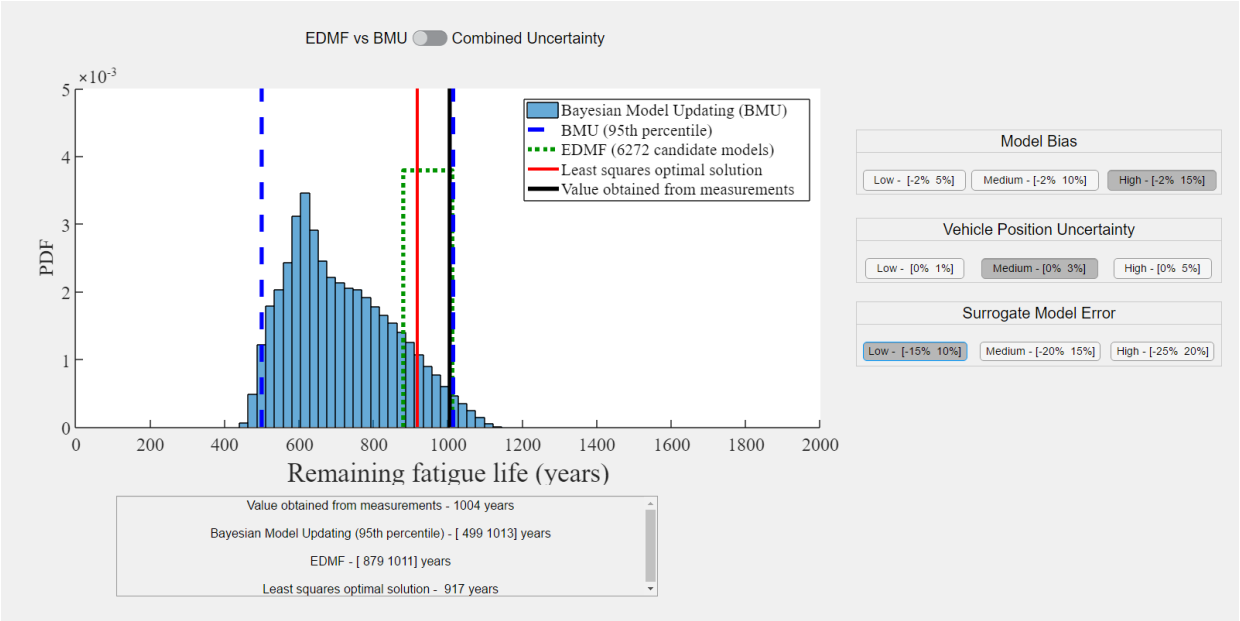

Figure 34 Low uncertainty scenario for surrogate modeling error

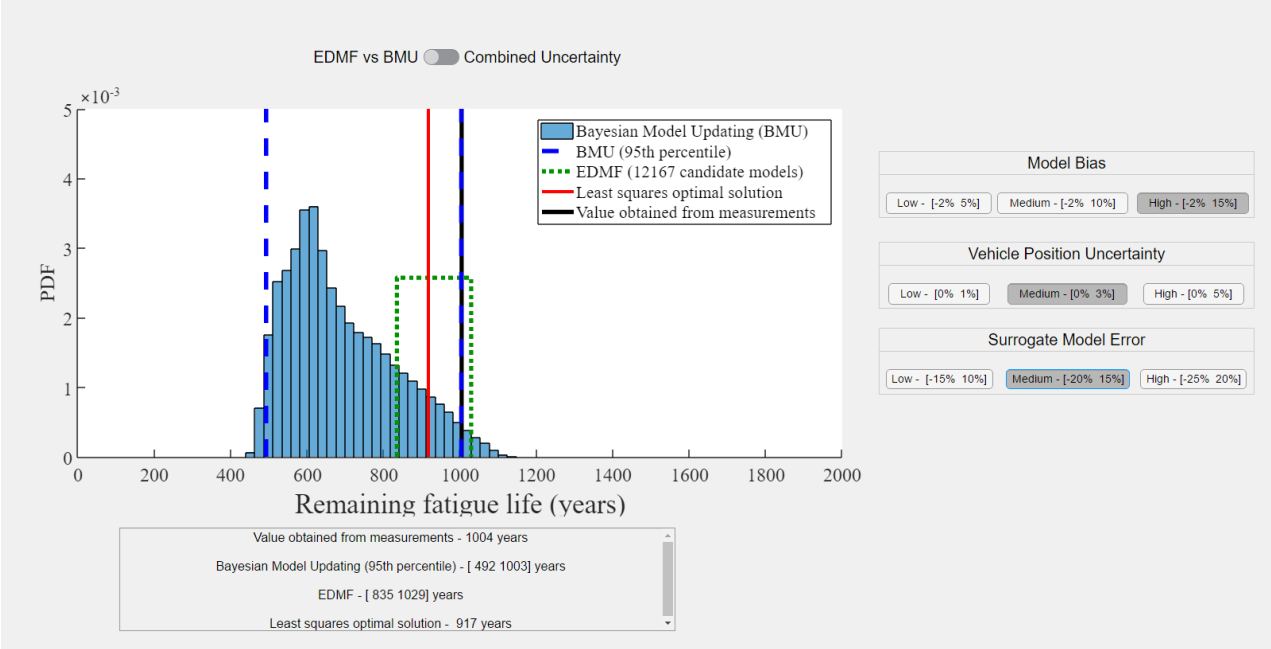

Figure 35 Medium uncertainty scenario for surrogate modeling error

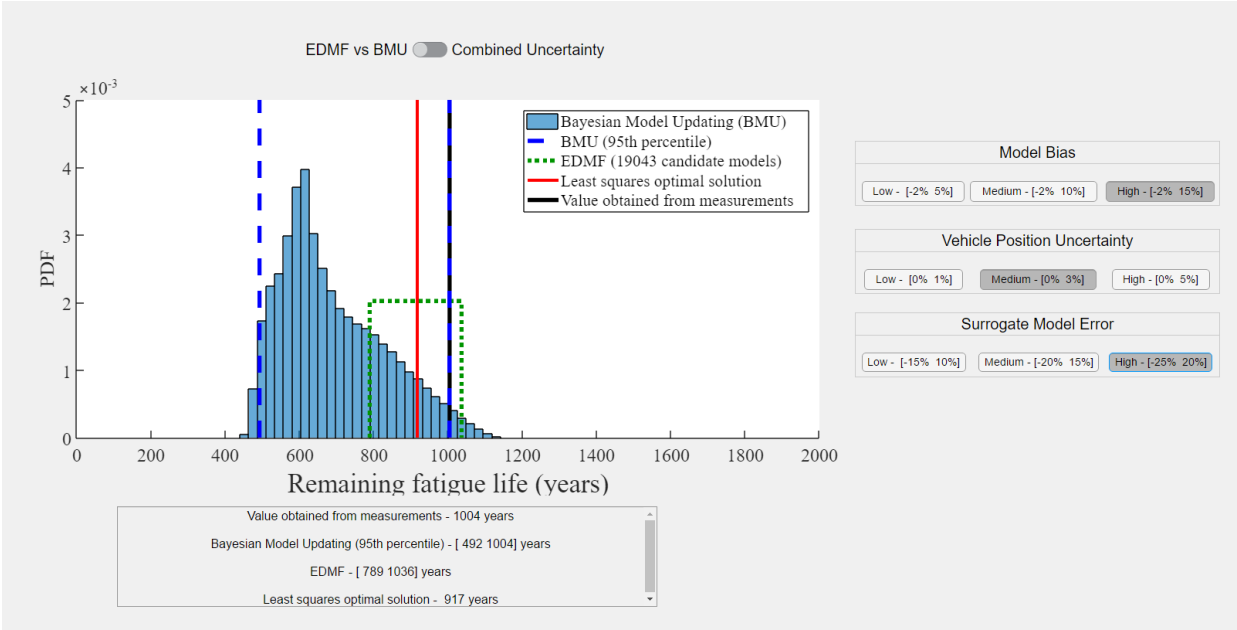

Figure 36 High uncertainty scenario for surrogate modeling error

6. Discussion

The models used in this study for fatigue life prediction are approximations of reality. Simplifications were made that induce systematic errors in prediction. When employing residual minimization, it is assumed that the difference between predictions and measurements is only dependent on the choice of parameter values and Gaussian uncertainty related to sensor noise. Therefore, variations to uncertainty estimation do not affect the results obtained with this methodology, as shown in section 4. Since models used for prediction are inevitably biased, inaccurate results are obtained when using this technique. This can be observed in Figure 22, where conservative predicitons are obtained for sensors B1 and B2 and an overestimation of RFL is obtained for sensors B3 and B4, when compared to the value computed with measurements. To obtain accurate predictions, modeling errors have to be taken into account and correctly estimated. Figures 21, 27 and 28 show that these errors do not follow a zero mean Gaussian distribution.

Studies have shown, through illustrative examples, that when in presence of systematic errors with unknown spatial correlations, BMU leads to biased results due to the wrong assumption of independence between uncertainties (Goulet and Smith 2013; Pasquier and Smith 2015). In this work, a large bias is obtained for results given by BMU, when compared to values computed with measurements and predictions using EDMF. Analyzing the model class used to update knowledge regarding the structure's behavior, it can be noticed that few of the parameters induce systematic error. In fact, KY1 is the only parameter present in the model class that can potentially lead to systematic errors. Parameters such as KYO, KXO, ROTZO and KX1 were considered as secondary parameters and assumptions made regarding their values introduced systematic errors in the model that are spatially correlated. When identifying using BMU, spatial independence was assumed, and thus biased results were obtained. Pai et al. (2017) predicted RFL for the Venoge bridge using a model class that contains a higher number of systematic error inducing parameters and obtained results with BMU that are less biased from the value computed with measurements, as can be observed in Figure 36. Nevertheless, using the model class presented in this study, EDMF provides with accurate results given that knowing the spatial relationship between uncertainties is not needed for this methodology.

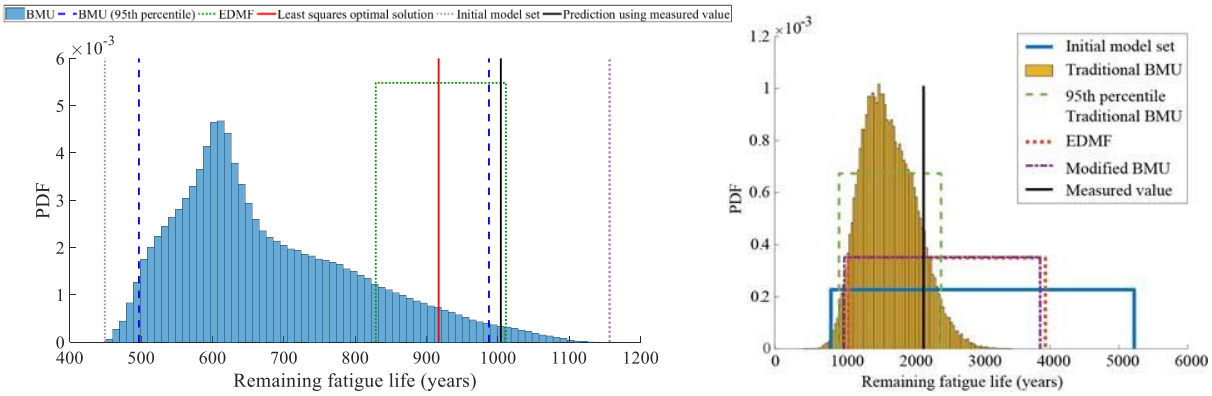

Figure 37 RFL prediction for sensor B1 (left) and RFL prediction for a cover plate detail (right) taken from Pai et al. (2017)

Apart from providing biased results, the BMU methodology does not indicate when uncertainties are being mis-evaluated. It was shown in section 5 that results given by BMU have negligible variation for different scenarios of uncertainty, and for wrong estimation of model bias. Spatial correlation between uncertainties also have an influence over results and by considering them as independent, minor changes were observed when taking different combinations of uncertainty. When using EDMF, it is not required to know the correlation between errors in order to obtain accurate predictions. Results are only dependent on the estimation of the combined uncertainty PDF. When this PDF is wrongly estimated, the methodology suggests a review on assumptions, as shown in section 5. For complex civil engineering structures, uncertainties are hard to estimate and spatial correlations between them can not be determined. EDMF provides a framework that enables iterative evaluation of uncertainties that are often hard to quantify, which can lead to better decision-making.
The procedure taken in this work followed the methodology proposed by Pasquier et al. 2016 for fatigue assessment of existing bridges and the toolbox described in chapter 5 can be used as a support for decision-making in the last step of the methodology, where the performance of the bridge is evaluated based on results obtained with data-interpretation.

It can be noted that the high computational time required to sample the posterior distributions, the need for substantial knowledge regarding modeling uncertainties and their correlations, and the overall complex nature of the methodology makes it hard for BMU to be implemented not only in the toolbox presented in this study, but also in a decision-making framework that is compatible with an engineer's *modus operandi*.

The aim of this study is to compare the applicability of three different data-interpretation techniques for fatigue-life prediction. Although being the first time that such comparison is made with regards to a full scale structure, future work is needed to verify this comparison with other cases as every civil infrastructure is unique due to its form, function and utility. Furthermore, albeit not considered in this study, further research can be made in the sense of including the effect of traffic evolution over time in the fatigue asssessment. In addition, the EDMF methodology can have several applications other than for fatigue analysis of structures. Ongoing work focuses on implementing EDMF in a framework for risk assessment of structures subjected to extreme events.

7. Conclusions

Three data-interpretation techniques were employed to predict remaining fatigue life of a highway bridge, a real case-study. Comparison of the results obtained with the methodologies are made with respect to accuracy when compared to predictions obtained from measurements. A GUI toolbox was developed to evaluate the robustness of each technique to variations in uncertainty estimation and aid in decision-making. The following conclusions can be made:

- Data-interpretation improves knowledge regarding the behavior of the bridge, increasing fatigue life prediction from 474 years to 863 years.
- EDMF provided with a wide yet robust prediction of equivalent stress range at sensor locations not used for identification. MLE of the posterior distribution obtained with BMU provided with results that are close to the value obtained with measurements for sensor C1, but biased for sensor C2. Prediction using the optimal parameter set obtained from residual minimization, when compared with the equivalent stress computed with measured values, is well corresponded for sensor C1 but biased for sensor C2. Results obtained from both BMU and residual minimization give an underestimation of equivalent stress range, which is not conservative.
- A large bias is obtained for prediction of RFL using BMU due to the assumption of independent spatial correlations between uncertainties while considering a lot of parameters that induce systematic errors as secondary parameters. EDMF allows for accurate predictions to be made with a simpler model class, i.e. a model class that does not include parameters that contribute to systematic errors.
- A thorough quantification of uncertainties and their spatial correlations is needed in order to obtain good results with BMU, which is an unfeasible task in the context of civil engineering. EDMF provides accurate results when there is little information regarding modeling errors.
- EDMF is a methodology that is simple to understand and employ while not requiring long computational time. Therefore, it is preferable to utilize this technique in applications that aid in decision-making, rather than BMU.

References

ANSYS. (2012). *ANSYS Mechanical APDL Element Reference*.

Bannantine, J. A., Comer, J. J., and Handrock, J. L. (1990). *Fundamentals of metal fatigue analysis*. *Englewood Cliffs, NJ, Prentice-Hall.*

Beck, J. L., and Katafygiotis, L. S. (1998). "Updating Models and Their Uncertainties. I: Bayesian Statistical Framework." *Journal of Engineering Mechanics*, American Society of Civil Engineers, 124(4), 455–461.

Box, G. E. P., and Behnken, D. W. (1960). "Some New Three Level Designs for the Study of Quantitative Variables." *Technometrics*, 2(4), 455–475.

CECM/TC6 n° 43 (1987). *"Recommandations pour la vérification à la fatigue des structures en acier." CTICM Centre technique et industriel pour la construction métallique.*

D 'angelo, L., and Nussbaumer, A. (2015). "Reliability based fatigue assessment of existing motorway bridge." *Structural Safety*, Elsevier Ltd, 57, 35–42.

Downing, S. D., and Socie, D. F. (1982). "Simple rainflow counting algorithms." (January), 31–40.

EN 1993 1-9 (2005). *"Eurocode 3: design of steel structures - Part 1-9: Fatigue." European Committee for Standardization (CEN)*.

Goulet, J. A., and Smith, I. F. C. (2013). "Structural identification with systematic errors and unknown uncertainty dependencies." *Computers and Structures*, Elsevier Ltd, 128, 251–258.

Jaynes, E. T. (2003). "*Probability theory: The logic of science*." *Cambridge university press.*

Mcfarland, J., and Mahadevan, S. (2008). "Multivariate significance testing and model calibration under uncertainty." 197, 2467–2479.

McKay, M. D., Beckman, R. J., and Conover, W. J. (1979). "Comparison of Three Methods for Selecting Values of Input Variables in the Analysis of Output from a Computer Code." *Technometrics*, Taylor & Francis, 21(2), 239–245.

Mottershead, J. E., Link, M., and Friswell, M. I. (2011). "The sensitivity method in finite element model updating : A tutorial." *Mechanical Systems and Signal Processing*, Elsevier, 25(7), 2275–2296.

Pai Sai; Nussbaumer, Alan; Smith, I. (n.d.). "Traffic-based condition assessment and fatigue-life predictions for a highway bridge." 320–327.

Pasquier, R., Asce, S. M., Goulet, J., Asce, A. M., Acevedo, C., Smith, I. F. C., and Asce, F. (2014). "Improving Fatigue Evaluations of Structures Using In-Service Behavior Measurement Data." 19(11), 1–10.

Pasquier, R., D. Angelo, L., Goulet, J.-A., Acevedo, C., Nussbaumer, A., and Smith, I. F. C. (2016). “Measurement, Data Interpretation, and Uncertainty Propagation for Fatigue Assessments of Structures.” *Journal of Bridge Engineering*, 21(5), 4015087.

Pasquier, R., and Smith, I. F. C. (2015a). “Sources and forms of modelling uncertainties for structural identification.” *SHMII 2015 - 7th International Conference on Structural Health Monitoring of Intelligent Infrastructure*.

Pasquier, R., and Smith, I. F. C. (2015b). “Robust system identification and model predictions in the presence of systematic uncertainty.” *Advanced Engineering Informatics*, 29(4), 1096–1109.

Pasquier, R., and Smith, I. F. C. (2016). “Iterative structural identification framework for evaluation of existing structures.” *Engineering Structures*, Elsevier Ltd, 106, 179–194.

Rutherford, B. M., Paez, T. L., Swiler, L. P., and Urbina, A. (2006). “Response Surface (Meta-model) Methods and Applications.” *24th Int. Modal Analysis Conf.(St. Louis, MO)*, 184–197.

SIA263 Code. (2003b). Norme SIA263: Steel structures, SIA, Zurich, Switzerland.

Šidák, Z. (1967). “Rectangular Confidence Regions for the Means of Multivariate Normal Distributions.” *Journal of the American Statistical Association*, Taylor & Francis, 62(318), 626–633.

Simoen, E., Papadimitriou, C., and Lombaert, G. (2013). “On prediction error correlation in Bayesian model updating.” *Journal of Sound and Vibration*, Elsevier, 332(18), 4136–4152.

Smith, I. F. C., Harris, D. K., and Smith, I. F. C. (2016). “Studies of Sensor Data interpretation for Asset Management of the Built environment.” 2(March), 1–9.

Yan, W.-J., and Katafygiotis, L. S. (2015). “A novel Bayesian approach for structural model updating utilizing statistical modal information from multiple setups.” *Structural Safety*, 52, Part B, 260–271.

Appendix A : Sample sensitivity analysis procedure for illustrative example

1. Define initial range for the structural parameters using engineering judgement (see table 1)
2. Box-Benkhen design of the structural parameters

Sample	E $[GPa]$	L $[mm]$	K $[Log(Nmm/rad)]$	I $[mm^4] \times 10^8$
1	30	8000	10.5	54
2	30	8500	10.5	54
3	40	8000	10.5	54
4	40	8500	10.5	54
5	35	8250	9	52
6	35	8250	9	56
7	35	8250	12	52
8	35	8250	12	56
9	30	8250	10.5	52
10	30	8250	10.5	56
11	40	8250	10.5	52
12	40	8250	10.5	56
13	35	8000	9	54
14	35	8000	12	54
15	35	8500	9	54
16	35	8500	12	54
17	30	8250	9	54
18	30	8250	12	54
19	40	8250	9	54
20	40	8250	12	54
21	35	8000	10.5	52
22	35	8000	10.5	56
23	35	8500	10.5	52
24	35	8500	10.5	56
25	35	8250	10.5	54
26	35	8250	10.5	54
27	35	8250	10.5	54

Table A1 Box-Benhken design of structural parameters for the illustrative example

3. Compute structural response for each location with the sample obtained from the Box-Benhken design
4. Multivariate linear regression with normalized design matrix

Appendix B : Stress time history for sensors B1, B2, B3 and B4

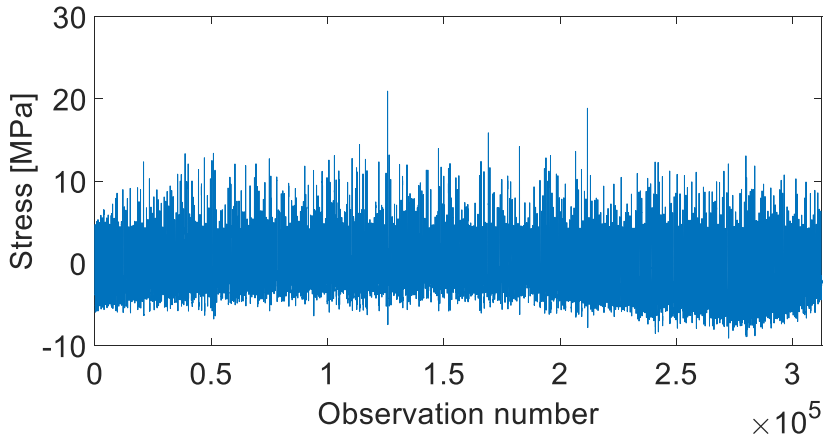

Figure A1 Stress time history for sensor B1

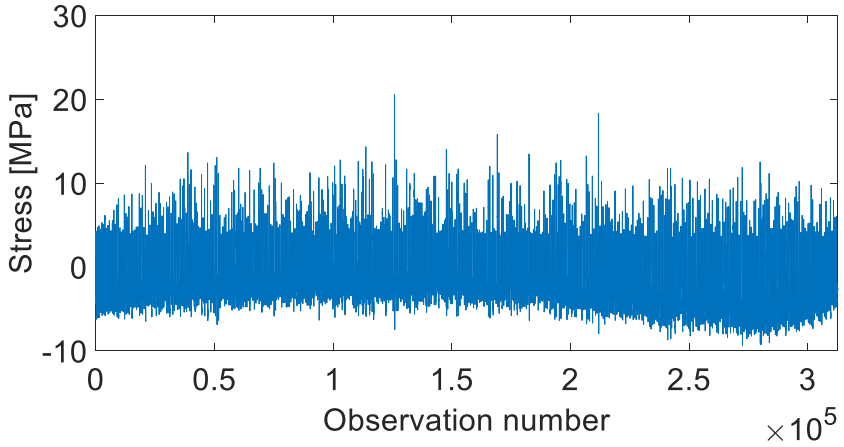

Figure A2 Stress time history for sensor B2

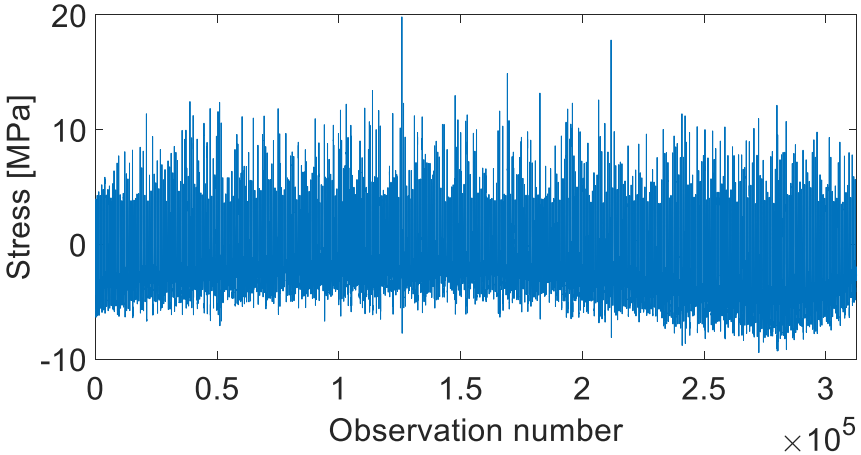

Figure A3 Stress time history for sensor B3

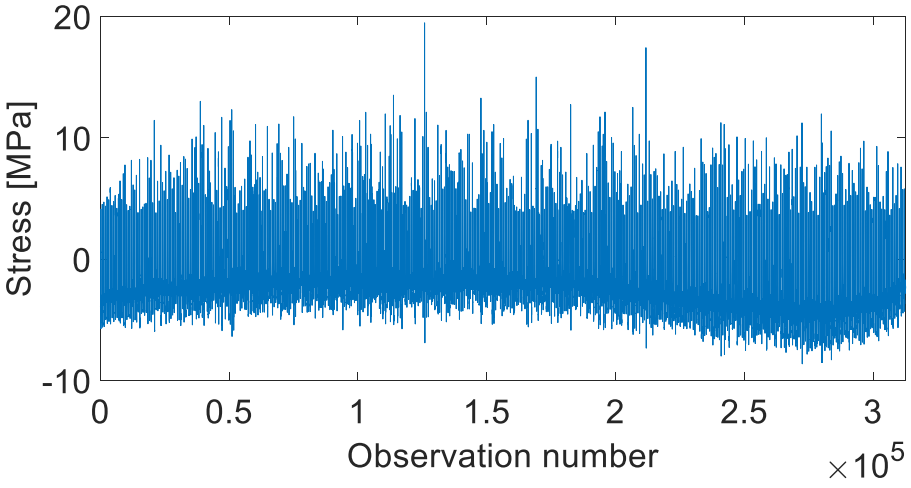

Figure A4 Stress time history for sensor B4

Appendix C : Stress histogram for sensors B1, B2, B3 and B4

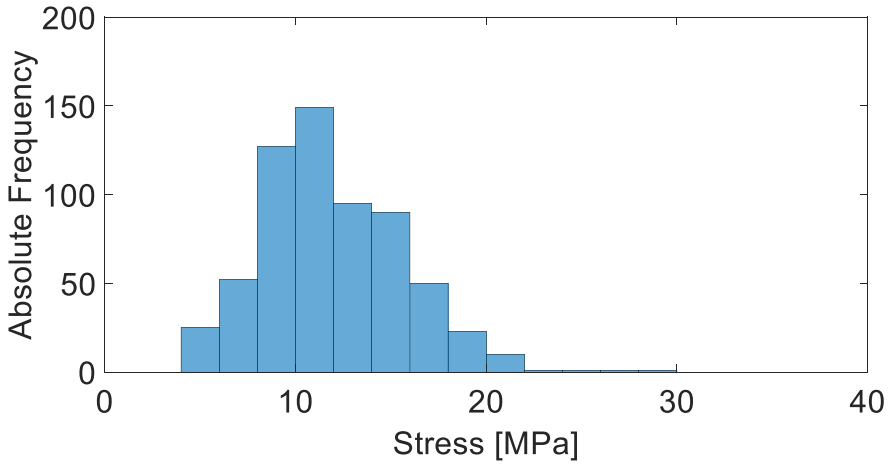

Figure A5 Stres histogram for sensor B1

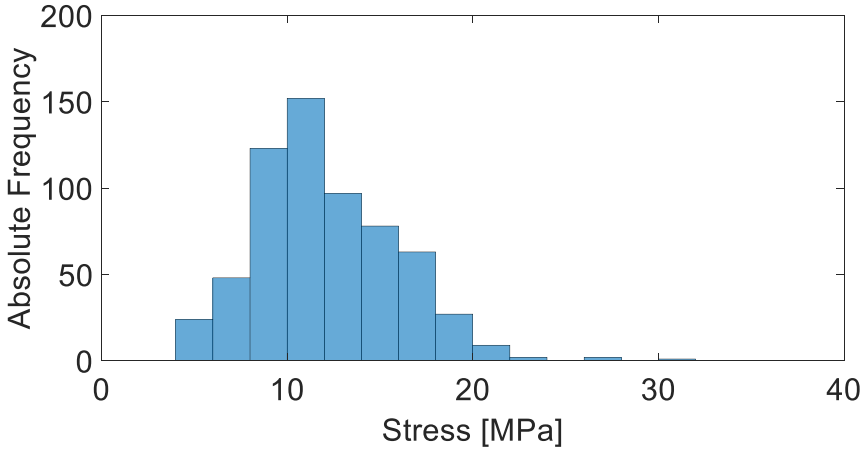

Figure A6 Stress histogram for sensor B2

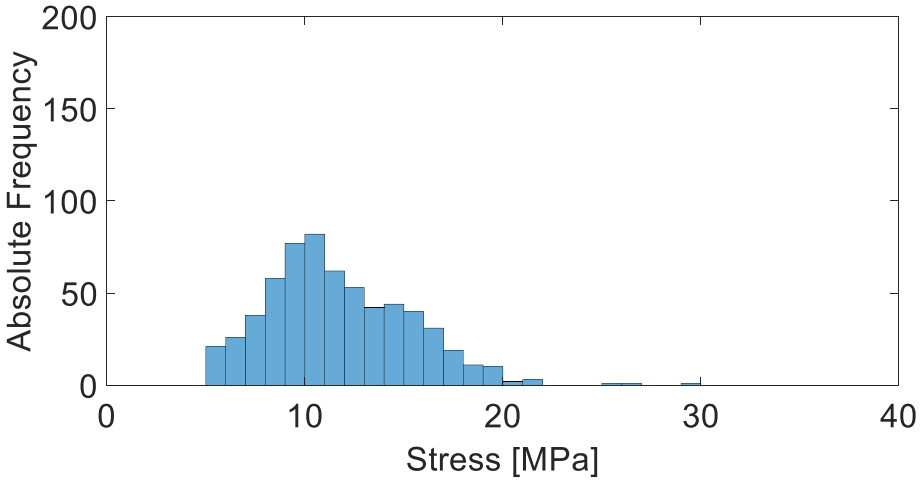

Figure A7 Stress histogram for sensor B3

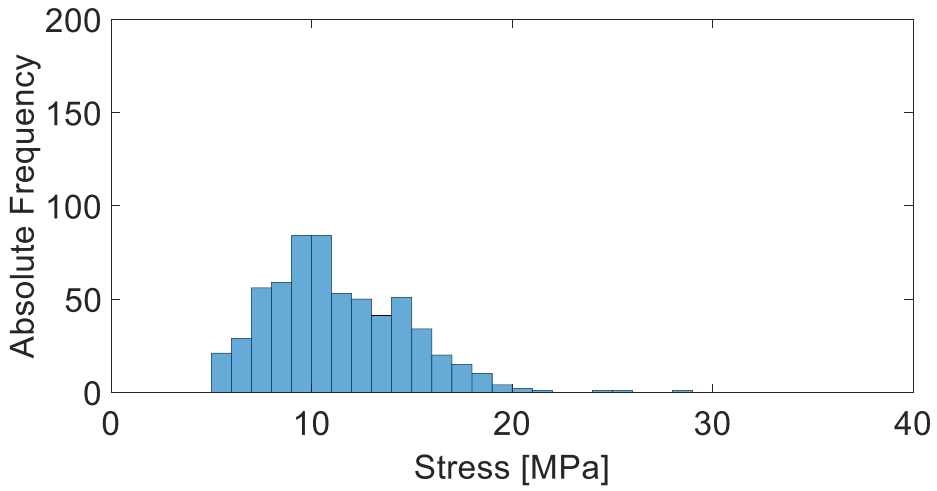

Figure A8 Stress histogram for sensor B4

Appendix D: Shape of influence lines for sensor locations and critical details

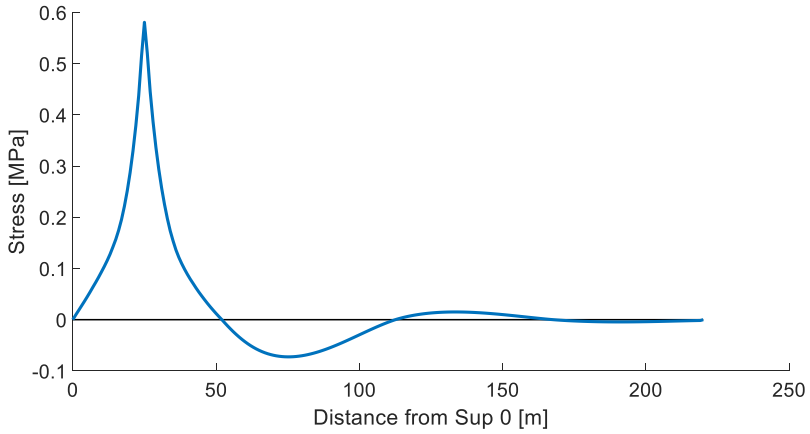

Figure A9 Representation of the shape of the influence line for sensor B1

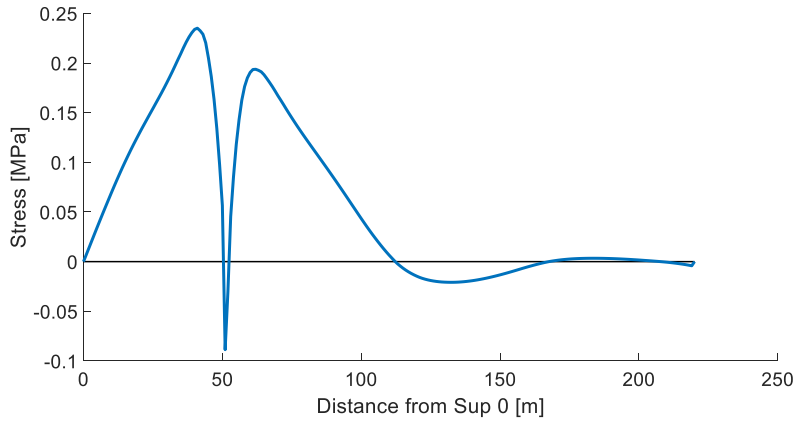

Figure A10 Representation of the shape of the influence line for sensor C1

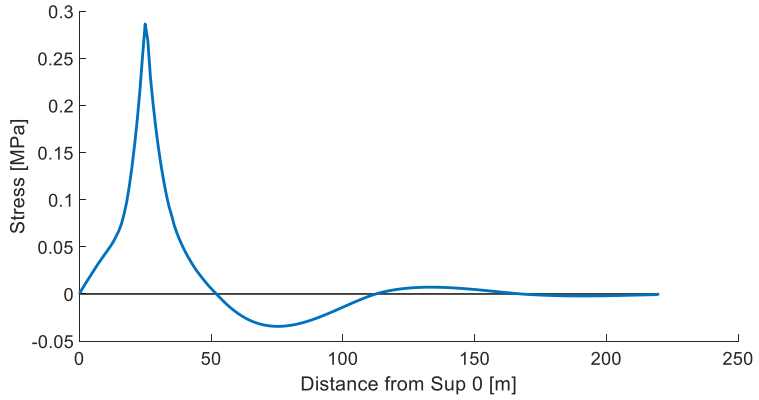

Figure A11 Representation of the shape of the influence line for CD1

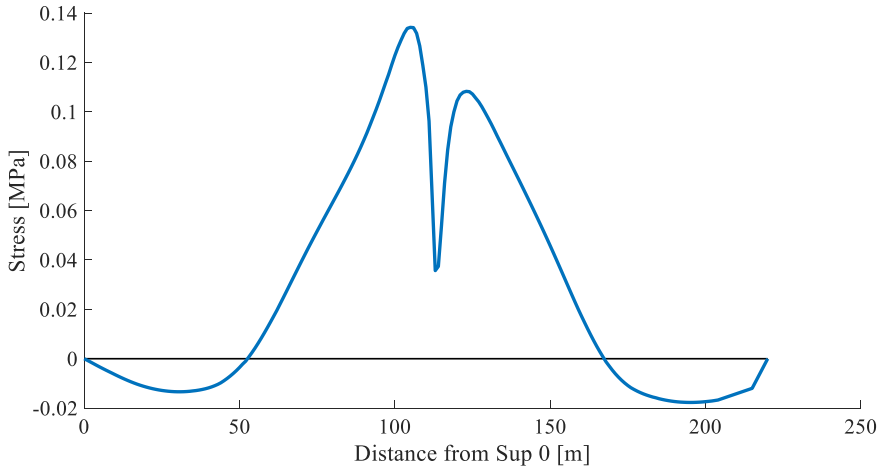

Figure A12 Representation of the shape of the influence line for CD2

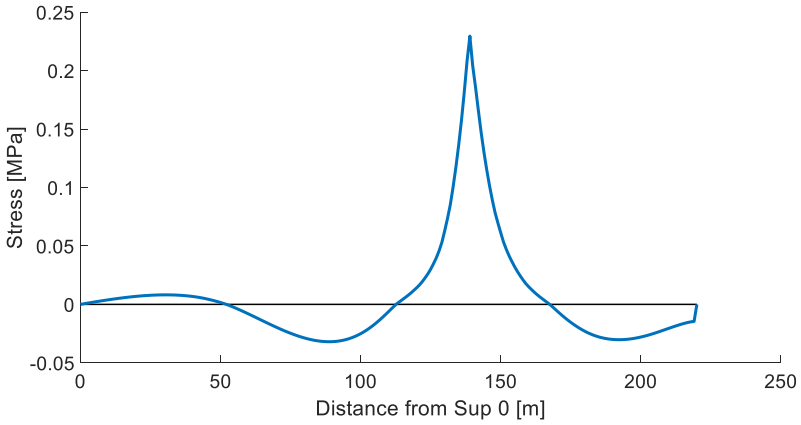

Figure A13 Representation of the shape of the influence line for CD3

Appendix E: Sample procedure for surrogate modeling

1. Generate latin hypercube sample of structural parameters

Sample	Ec $[GPa]$	KdeckX $[Log\ (Nmm)]$	KdeckZ $[Log(Nmm)]$	KY1 $[Log(Nmm)]$
1	36212.22	6.360447	5.921643	6.458769
2	24286.3	5.693321	6.106158	5.708063
3	27628.23	4.513861	6.549905	7.300782
4	26267.06	6.311966	5.11691	6.430263
5	32569.25	5.042873	6.121633	6.044479
6	38700.44	4.086757	5.517187	6.18372
7	24048.4	4.554098	5.092187	6.532549
8	33756.33	6.267888	5.304685	6.360956
9	28772.86	6.135968	6.078461	7.096563
10	34046.67	5.540781	4.644747	6.999068
11	37159.64	5.495817	6.897168	5.529235
12	24480.59	4.008174	6.882851	5.66282
13	38535.27	4.329645	4.862656	6.451025
14	20348.44	4.500774	4.995504	7.286165
15	29826.67	6.082961	6.998179	7.422684
16	37436.73	5.067123	6.338645	6.919524
17	23056.44	4.865163	6.347272	6.236288
18	27519.25	4.663584	5.873644	7.60919
19	25819.98	4.789956	6.391938	5.967647
20	29869.59	5.199203	5.363321	5.63054
21	35757.64	4.446394	6.457134	7.171442
22	26673.92	5.50602	4.358576	7.251635
23	31052.25	5.682493	5.497541	7.667308
24	39221.1	5.762509	6.143081	7.259444
25	35912.33	5.006341	4.689283	7.820836
26	35264.97	6.397087	5.545013	6.653463
27	39011.98	4.612014	5.12014	7.85896
28	23437.82	5.928766	6.350951	7.923616
29	31860.75	5.088156	6.014248	6.638547
30	33470.99	6.113454	6.932335	7.514505
31	35573.95	5.021828	6.742532	7.659746
32	32160.8	5.822661	5.693047	7.774415

33	25917.34	4.956834	4.193227	6.447658
34	20689.76	6.173939	5.237176	7.245375
35	22308.9	5.941536	4.524181	7.803175
36	25234.58	5.218724	6.973811	7.404918
37	36106.55	5.120792	5.501858	7.764513
38	37711.08	5.027316	6.61984	6.421527
39	28048.83	5.251991	5.967856	7.471816
40	39815.48	5.056092	5.410121	7.940864
41	20583.97	4.148386	4.241827	6.248906
42	36402.58	5.249465	6.873679	5.819918
43	28871.76	5.596455	5.833179	7.444532
44	39581.72	4.819149	4.421918	6.776325
45	36918.45	5.125189	5.187203	7.870835
46	22916.53	4.270403	6.60335	6.57244
47	26183.53	5.324635	5.609707	5.981919
48	21384.03	4.761815	5.614556	7.007927
49	27971.45	4.04768	5.33471	7.756452
50	27744.94	6.203815	4.531268	6.888609
51	25758.85	4.496306	4.698124	6.136935
52	38253.74	5.757357	4.840685	6.578586
53	28546.13	4.3885	5.530236	6.310177
54	32867.62	6.42696	5.666688	5.670081
55	31723.43	5.392347	5.253763	6.799078
56	35943.13	6.219228	6.704729	7.594661
57	24917.43	5.841911	4.905409	6.6994
58	34238.87	5.390615	5.976414	6.063618
59	27045.17	5.602947	4.856657	7.647606
60	21304.4	4.98011	4.729168	7.343821
61	36711.51	5.453647	5.046096	7.282775
62	39526.74	6.015014	6.377607	6.827024
63	22155.26	4.696717	5.595137	6.731327
64	28730.04	4.772165	5.712999	6.073076
65	33986.6	4.972029	4.658627	6.6749
66	21966.72	6.155225	4.271735	7.957229
67	20648.31	4.224039	5.930699	6.539922
68	27838.69	4.470823	6.911713	7.048215
69	22560.2	4.801526	4.26515	6.500785

70	39463.39	4.997137	4.543402	7.214352
71	38607.55	5.854179	4.025436	5.899191
72	38342.78	6.215683	6.475815	5.943476
73	39727.66	4.111871	5.449657	5.686104
74	32454.84	4.187371	5.420732	7.119894
75	32732.44	4.038706	6.719566	7.563802
76	26427.33	4.451139	5.265239	7.319247
77	21419.48	4.072133	5.626143	7.206387
78	27882.74	5.304526	6.094659	5.697433
79	29319.07	4.606349	4.180018	6.630356
80	29202.26	6.318574	5.480975	7.523194
81	34501.04	5.839388	5.459852	7.502689
82	30662.5	5.353958	6.512195	6.268867
83	38854.77	4.178907	5.815147	6.016583
84	31177.45	5.459388	4.326098	5.722034
85	37074.63	5.717187	5.791769	7.064667
86	22397.15	5.616261	4.461256	6.708937
87	35309.64	5.18351	5.200016	5.535308
88	39623.95	4.303064	5.558043	6.321838
89	24344.81	6.057728	6.5913	6.402617
90	38197.03	4.639901	5.986925	7.310843
91	31947.28	5.413668	6.325888	7.461747
92	33129.92	6.029778	4.341837	6.78365
93	32246.9	5.418682	5.526317	5.751822
94	34981.86	4.792369	6.675738	6.81218
95	28939.1	6.128085	4.309088	7.165882
96	33892.97	4.125367	5.883325	6.35095
97	28633.19	5.868707	4.202687	5.889521
98	37817.56	6.253949	5.226992	5.996137
99	22459.19	5.292916	6.13662	7.972243
100	36274.37	5.309866	4.252657	6.51036
101	23298.03	4.382232	6.380145	7.451643
102	34199.63	6.418661	5.913012	6.834974
103	28255.81	6.161523	6.659101	7.426028
104	30782.51	5.346686	5.855293	7.840938
105	26264.08	5.134656	5.243646	6.952767
106	26954.53	4.324681	5.954747	6.904146

107	33331.45	6.340865	5.468587	6.93887
108	39100	4.008766	4.237245	5.603429
109	37034.62	4.438367	5.900129	7.797067
110	30848.1	4.878898	6.82205	7.681611
111	39293.97	4.100803	5.430667	7.081149
112	31247.51	4.363833	5.786516	6.090845
113	34338.67	5.861134	5.727909	6.165416
114	37666.26	5.327272	4.633196	5.655658
115	24229.03	4.931475	5.996446	6.620047
116	21775.42	4.562038	4.435616	6.865386
117	35841.91	5.27954	6.290912	7.182811
118	27465.25	4.428248	4.581664	5.508268
119	33154.18	4.887133	4.486086	5.810214
120	38496.36	4.679014	6.17266	6.47765
121	25282.3	6.097616	4.737093	6.223996
122	25480.58	5.792675	4.457079	7.82734
123	29450.23	4.900529	5.867032	7.781985
124	29586.68	5.526615	4.709752	7.848999
125	31375.54	4.725258	4.760822	5.877657
126	30418.7	4.670631	6.48314	5.79046
127	22858.31	4.657393	5.167657	6.766185
128	27304.67	5.727915	4.285026	6.807209
129	26398.91	5.448409	4.552094	7.091543
130	21661.93	4.167859	5.086198	6.081757
131	24419.31	4.117143	6.587814	6.291076
132	39946.47	4.649138	5.772773	6.149685
133	37939.32	5.239196	4.752272	5.730768
134	34539.19	4.718341	5.053067	5.679036
135	22691.36	5.746319	6.633803	6.680054
136	29524.57	6.379229	6.682377	6.116707
137	21129.19	5.974754	5.354885	7.963003
138	32014.83	5.636895	4.786706	7.140405
139	35683.86	5.945229	5.639987	6.768516
140	38024.94	5.918819	4.514194	7.127157
141	22751.39	5.549362	6.538282	7.915936
142	25453.13	5.960107	4.668051	6.34608
143	34413.67	5.098388	4.478497	7.730893

144	28401.7	5.578909	4.064946	7.654943
145	29371.99	4.625632	4.959826	7.488081
146	36983.62	4.750116	5.645288	5.576073
147	39767.99	4.050206	6.439539	6.194106
148	20155.4	4.964127	6.365577	6.041548
149	26076.51	4.34372	4.058364	6.916462
150	29070.31	5.156614	5.104279	5.748025
151	33658.08	4.367822	5.471817	6.253348
152	39353.56	6.086185	5.409147	7.567282
153	32527.99	5.890815	4.147672	5.96388
154	25126.43	4.245163	5.82754	5.554641
155	38924.59	6.058638	5.706481	7.999174
156	37899	4.542959	4.885909	6.852374
157	28167.88	4.293724	5.318858	5.935653
158	33370.27	5.702475	4.385928	6.385146
159	29746.79	6.389611	4.893241	7.19215
160	39898.07	6.049667	6.27457	6.74127
161	26622.08	5.629482	4.116429	6.39333
162	37234.44	4.899022	4.793384	6.84611
163	37511.15	4.706987	6.983213	5.839341
164	26582.75	5.213169	5.348684	7.399627
165	33201.75	4.986116	4.415604	7.435104
166	38115.71	6.175224	6.620628	6.550841
167	37747.34	4.02267	4.094298	7.226869
168	21700.2	5.803905	4.314224	6.293021
169	20511.95	4.917244	4.712354	7.155463
170	29958.91	4.831944	6.26753	5.78174
171	20132.87	5.651756	6.663061	6.596846
172	23729.14	6.332475	4.627051	6.989531
173	20205.33	6.22597	6.034293	5.774821
174	34672.92	6.487315	6.413652	5.614223
175	23544.56	4.150216	6.806011	6.15633
176	38939.09	4.335366	6.577511	6.414978
177	34288.06	6.435645	5.150647	7.238765
178	35348.2	4.216645	6.755511	5.73719
179	27553.76	5.773287	5.324682	7.707297
180	25386.74	6.34783	4.443652	5.915061

181	32103.17	4.357667	4.923319	6.279262
182	36347.41	6.193872	6.05561	6.338275
183	36799.87	4.059811	6.73827	7.893876
184	37562.96	4.938805	6.783056	5.830834
185	36171.12	4.582199	5.760751	7.601607
186	28396.11	6.444451	6.796294	6.684053
187	28503.87	6.11808	5.213612	6.126957
188	21477.36	6.00272	4.131103	7.688882
189	28092.12	6.248838	4.875171	6.660672
190	30350.56	5.980176	4.103702	6.47472
191	22004.29	6.10268	6.55535	7.386536
192	26044.98	4.870701	5.288908	6.215732
193	25016.93	5.89185	4.228869	7.891245
194	30075.14	5.714436	4.398921	6.72454
195	27704.45	4.734442	4.675543	7.274782
196	27165.23	4.913552	4.600612	7.008705
197	21223.16	6.290528	6.563662	5.86229
198	24968.73	4.082644	6.280703	7.477031
199	24721.11	5.78551	5.009371	7.578418
200	32784.93	4.488566	5.136931	5.568842
201	31639.2	6.071829	5.730502	6.872338
202	22265.65	4.522482	5.589896	6.017932
203	22483.29	4.255879	4.988322	7.220886
204	21595.86	5.622835	6.502447	6.56571
205	33437.89	4.279471	4.771662	7.334898
206	29697.15	6.016768	6.723941	6.644443
207	36025.99	6.263458	5.144821	6.821818
208	21904.25	4.850473	6.060571	5.902343
209	24861.26	4.715275	4.812588	6.229845
210	21181.07	4.025625	4.072989	6.057867
211	31595.12	5.377047	6.762553	7.545125
212	25151.33	6.451195	5.561262	7.905843
213	32843.57	5.878313	6.020359	6.896587
214	22623.19	4.849105	5.800181	7.628449
215	28834.55	5.571204	6.240814	7.930703
216	20974.49	5.986212	6.927165	6.948772
217	21844.87	4.316187	6.189414	7.350071

218	28326.46	5.524823	6.52179	6.307438
219	32975.31	6.147585	6.968205	6.522215
220	30574.84	5.775571	6.259651	5.624684
221	23834.55	4.595717	4.402287	7.35898
222	30946.96	4.942706	4.974595	6.17189
223	32620.57	5.471849	4.086685	7.52509
224	25543.35	4.134296	6.084218	7.945471
225	35099.18	5.145544	6.841455	6.545306
226	23343	4.567562	6.193576	6.181768
227	24568.97	5.36581	6.235799	5.589871
228	30315.68	6.0399	4.494541	7.745956
229	36624.7	5.03582	5.028177	7.114837
230	35429.15	5.438655	5.687637	6.375526
231	30163.92	4.241655	5.387946	7.88102
232	20040.45	6.296797	6.467403	7.142057
233	38771.97	4.480665	6.400574	6.959876
234	34790.86	5.063389	4.963584	6.60542
235	26780.52	5.690156	5.391709	7.591487
236	36866.18	5.956589	6.046112	5.597158
237	31871.15	4.411719	5.748316	6.496797
238	24626.05	5.428379	4.372599	6.099223
239	23073.88	6.473563	4.031272	5.850256
240	36571.95	5.825558	4.336445	5.765083
241	25706.65	4.207865	4.618212	7.698628
242	25629.74	4.098319	5.370036	5.645775
243	26893.58	5.370765	5.570409	7.854098
244	34099.58	5.268673	6.95844	7.107904
245	22960.85	5.34045	6.150711	5.546942
246	32391.15	4.400574	6.905754	5.520127
247	31415.89	5.01315	4.167769	7.550044
248	35623.26	6.191196	5.898636	6.488041
249	26509.93	5.902715	6.857398	7.4942
250	22112.49	5.164335	4.804555	5.924863
251	36515.05	6.276833	6.819178	7.382062
252	33056.7	4.22531	6.694019	5.950837
253	30044.38	4.419265	4.569708	7.982947
254	33544.46	6.370846	6.225451	7.791422

255	33851.09	4.265841	4.506675	6.703546
256	29662.05	5.080935	4.290563	7.722163
257	35033.68	4.745516	4.946969	6.931506
258	31791.86	4.166572	5.015718	7.292467
259	29173.16	4.46431	5.19339	6.744308
260	32327.25	5.170087	4.836189	5.846903
261	39151.96	4.7819	4.938638	7.713324
262	31110.51	5.815249	6.169034	6.614959
263	35495.58	4.58603	6.776948	7.989686
264	23489.7	6.403587	4.211761	6.259297
265	33689.83	4.837069	4.823727	5.867323
266	24153.28	4.391938	5.757941	7.185153
267	27246.59	5.48643	6.440198	6.106317
268	34660.97	5.997295	6.315622	5.711803
269	26824.44	5.262325	5.651648	7.623318
270	20915.57	6.476126	4.124608	7.073941
271	23740.38	5.225049	6.009749	7.810936
272	20846.65	4.809679	6.499932	6.325744
273	31285.66	4.622105	4.172139	7.410409
274	24777.98	6.410422	5.065526	7.368142
275	27375.68	4.525505	4.747113	6.206457
276	23160.51	5.102766	5.291368	7.738444
277	37272.99	4.537657	4.913438	6.029844
278	25982.36	4.689282	6.867153	5.792202
279	23870.01	5.178374	4.363554	6.440787
280	34817.42	6.497197	4.597364	5.928906
281	20333.04	6.300337	6.648252	5.51149
282	20743.28	5.479649	5.846314	6.880997
283	29020.3	5.55865	5.174625	6.981685
284	38429.17	4.194363	5.030736	6.971597
285	30710.82	5.510783	5.942509	7.021978
286	30511.15	6.233686	6.218523	7.540317
287	31528.18	5.283834	6.209971	5.559221
288	38302.78	5.109719	6.83873	7.029663
289	24089.52	4.290373	4.150831	6.752747
290	37361.87	5.659746	5.273279	7.05658
291	21039.86	6.462799	4.018862	7.63774

292	35137.69	5.739178	6.110398	6.007917
293	20442.63	5.203972	6.308806	5.637534
294	27070.15	5.66807	5.675076	6.114419
295	30264.66	5.553841	4.046387	7.327632
296	23637.26	5.914501	4.0053	6.585433
297	34886.62	5.64705	6.949412	6.371736
298	23953.13	5.406777	4.5767	5.803676
299	23232.66	6.355411	6.427355	5.985565
300	30892.52	5.590086	5.077541	7.03657

Table A2 Latin hypercube sample of structural parameters

2. Compute structural response for each location with the generated sample
3. Train neural network for each location with the sample generated as input and structural response as target

Appendix F : Source code for the GUI toolbox developed

```
classdef Venoge < matlab.apps.AppBase
    % Properties that correspond to app components
    properties (Access = public)
        UIFigure                          matlab.ui.Figure
        UIAxes                            matlab.ui.control.UIAxes
        Label                             matlab.ui.control.Label
        Label_2                           matlab.ui.control.Label
        Switch                            matlab.ui.control.Switch
        ModelBiasButtonGroup              matlab.ui.container.ButtonGroup
        MbiasLow                          matlab.ui.control.ToggleButton
        MbiasMed                          matlab.ui.control.ToggleButton
        MbiasHigh                         matlab.ui.control.ToggleButton
        VehiclePositionUncertaintyButtonGroup  matlab.ui.container.ButtonGroup
        VehicleLow                        matlab.ui.control.ToggleButton
        VehicleMed                        matlab.ui.control.ToggleButton
        VehicleHigh                       matlab.ui.control.ToggleButton
        SurrogateModelErrorButtonGroup    matlab.ui.container.ButtonGroup
        SurrLow                           matlab.ui.control.ToggleButton
        SurrMed                           matlab.ui.control.ToggleButton
        SurrHigh                          matlab.ui.control.ToggleButton
        TextArea                          matlab.ui.control.TextArea
    end
    properties (Access = private)
        ucbounds
        comb
        mi
        ma
        res
        par
        uncertaindist
        sensorfatlife
        Param
        T_low
        T_high
        CM
        Bayesdist

    end
    methods (Access = private)

        function makehist(app,distr)
            histogram(app.UIAxes,distr,'Normalization','pdf','NumBins',30);

        end

        function setaxis(app)
            set(app.UIAxes,'fontsize',24)
            if strcmp(app.Switch.Value,'Combined Uncertainty')
                app.UIAxes.XLim=[-100 100];
                app.UIAxes.YLim=[0 0.045];
```

```
            xlabel(app.UIAxes,'Combined uncertainty (%)','FontSize',16)
            ylabel(app.UIAxes,'PDF','FontSize',16)
        else
            app.UIAxes.XLim=[0 2500];
            app.UIAxes.YLim=[0 0.005];
            xlabel(app.UIAxes,'Remaining fatigue life…
            (years)','FontSize',16)
        end
        end

    function combineuc(app)

          bounds{2}=[-2  10  ;              %model bias
                      0   3  ;              %vehicle position
                     -20 15];               %surrogate
          bounds{1}= [-2  5  ;              %model bias
                     0   1  ;               %vehicle position
                     -15 10];


         bounds{3}=[-2  15  ;           %model bias
                    0   5  ;            %vehicle position
                    -25 20];              %surrogate

          uncertainties = [-1.2  2.2  ;              %secondary
                           -1  3   ;                %traffic load
                           0  0.5 ;                %measurement error
                        bounds{app.comb(1)}(1,:);
                        bounds{app.comb(2)}(2,:);
                        bounds{app.comb(3)}(3,:)];
            for i=1:size(uncertainties,1)

                if i==3
                   generated(:,i)=-random('normal',uncertainties(i,1),uncer-
tainties(i,2),[1E6,1]);
                else
                   generated(:,i)=random('unif',uncertainties(i,1),uncertain-
ties(i,2),[1E6,1]);
                end

            end
        app.uncertaindist=sum(generated,2);
    end

    function calcEDMF(app)
        app.CM=0;
        n_m=4;
        nsamples=1E5;
        nvar=4;
        nb_space=round((nsamples)^(1/nvar));
        par_samp=zeros(nb_space,nvar);
         app.Param.bound=[20000 40000; 4 6.5; 4 7; 5.5 8];
         P_min=app.Param.bound(:,1)';
        P_range=transpose(app.Param.bound(:,2)-app.Param.bound(:,1));
```

```
            for i=1:nvar
            par_samp(:,i)=linspace(P_min(i),P_min(i)+P_range(i),nb_space);
            end
            par_r = f_grid_sampling(par_samp,nb_space,nvar, 3);
            app.par=par_r;
            m_u=f_resp_EDMF(par_r);
            m_y(:,1)=app.sensorfatlife(1);
            m_y(:,2)=app.sensorfatlife(2);
            m_y(:,3)=app.sensorfatlife(3);
            m_y(:,4)=app.sensorfatlife(4);
            m_r=100*(m_u repmat(m_y,[nb_space^nvar,1])./rep-
mat(m_y,[nb_space^nvar,1]);
            app.T_low= prctile(app.uncertaindist,100*0.5*(1-0.95^(1/n_m)));
            app.T_high= prctile(app.uncertaindist,100*0.5*(1+0.95^(1/n_m)));
            EDMF_r = f_EDMF(m_r,app.T_low,app.T_high);
            EDMF_r= sortrows([EDMF_r par_r m_r],-1);
            app.CM=EDMF_r(EDMF_r(:,1)==1,2:end);

            end



        function updateplot(app)
            cla(app.UIAxes)
            hold(app.UIAxes,'on')
            if strcmp(app.Switch.Value,'Combined Uncertainty')
                makehist(app,app.uncertaindist)
                plotBounds(app)


            else

                plotEDMFvsBayes(app)
                perc=[prctile(app.Bayesdist,2.5),prctile(app.Bayesdist,97.5)];
                if app.comb==[2 2 2]
                    perc(2)=987;
                end
app.TextArea.Value= {sprintf('Value obtained from measurements - %4.0f
years',app.sensorfatlife(1));...
                    sprintf('\nBayesian Model Updating (95th percentile) - [%4.0f
%4.0f] years',perc(1),perc(2))...
                    ;sprintf('\nEDMF - [%4.0f %4.0f]
years',app.mi,app.ma);sprintf('\nLeast squares optimal solution - %4.0f
years',app.res) }
                end
            setaxis(app)
        end

        function plotBounds(app)

            xBoundslow = [app.T_low, app.T_low];
            xBoundshigh = [app.T_high, app.T_high];
            yBounds = [0, 0.03];
            plot(app.UIAxes,xBoundslow, yBounds,'r--','linewidth', 3);
```

```
            plot(app.UIAxes,xBoundshigh, yBounds,'r--','linewidth', 3);
            text(app.UIAxes,app.T_low-6.5,0.032,'Tlow','FontSize',24)
            text(app.UIAxes,app.T_high-5,0.032,'Thigh','FontSize',24)
            leg=legend(app.UIAxes,'Combined uncertainty','Location','northeast');
            set(leg,'visible','off')
            plot(app.UIAxes,[0,0],[0,0.045],'k--','linewidth',3)
        end

        function plotEDMFvsBayes(app,CM)

                set(app.UIAxes,'fontsize',24)
                app.ma=max(surr_b1(app.CM(:,1:4)));
                app.mi=min(surr_b1(app.CM(:,1:4)));
                x_CM=[app.mi, app.mi, app.ma, app.ma];
                yp=0.5/(app.ma-app.mi);
                y_CM=[0, yp, yp, 0];
                clear posterior
                load(num2str(app.comb))
                app.Bayesdist=posterior;
                xprct=[prctile(posterior,2.5),prctile(posterior,2.5),prctile(pos-
terior,97.5),prctile(posterior,97.5)];
                        bay=histogram(app.UIAxes,app.Bayesdist,'Normaliza-
tion','pdf','NumBins',30);
                ed=plot(app.UIAxes,x_CM, y_CM,':','color',[0    0.58    0],'lin-
ewidth',4,'Visible',vis)
                real=plot(app.UIAxes,[app.sensorfatlife(1), app.sensorfat-
life(1)],[0, 1],'k','linewidth',4)
                perc=plot(app.UIAxes,[xprct(1),xprct(1)], [0,0.034],'b--','lin-
ewidth',4);
                if app.comb==[2 2 2]
                    xprct(3)=987;
                end
                plot(app.UIAxes,[xprct(3),xprct(3)], [0,0.034],'b--','lin-
ewidth',4);

                rsm=plot(app.UIAxes,[app.res,app.res],[0,0.034],'r','linewidth',3)
                if strcmp(app.Switch.Value,'EDMF vs BMU')
                lg=legend(app.UIAxes,[bay,perc,ed,rsm,real],{'Bayesian Model Up-
dating (BMU)','BMU (95th percentile)',sprintf('EDMF (%i candidate mod-
els)',num),'Least squares optimal solution',...
                    'Value obtained from measurements'},'Location','northeast')
                set(lg,'FontSize',10)
                end
        end

        function resmin(app)
            pred=[surr_b1(app.par) surr_b2(app.par) surr_b3(app.par)
surr_b4(app.par)];
            eo=(pred-repmat(app.sensorfatlife(1:4),[size(pred,1) 1])).^2;
            w=diag(app.sensorfatlife(1:4).^(-2));
            for i=1:size(eo,1)
                    res(i,1)=eo(i,:)*w*eo(i,:)';
            end
```

```
            for i=1:size(pred,1)
                res(i,1)=sum((pred(i,:)-app.sensorfatlife(1:4)).^2);
            end
            [mini pos]=min(res);
            resCM=app.par(pos,:);
            rfl_res=[surr_b1(resCM) surr_b2(resCM) surr_b3(resCM) surr_b4(resCM)];
            app.res=rfl_res(1,1);
        end

    end
    methods (Access = private)
        % Code that executes after component creation
        function startupFcn(app)

            load('SensorData.mat')
            app.sensorfatlife=sensorfatlife;

            app.Switch.Value= 'Combined Uncertainty';
            app.comb=[2 2 2];
            app.ModelBiasButtonGroup.SelectedObject=app.MbiasMed;
            app.VehiclePositionUncertaintyButtonGroup.SelectedObject=app.Vehi-
cleMed;
            app.SurrogateModelErrorButtonGroup.SelectedObject=app.SurrMed;

            combineuc(app)
            calcEDMF(app)
            resmin(app)
            updateplot(app)
            app.TextArea.Visible='off';
        end
        % Selection changed function: ModelBiasButtonGroup
        function ModelBiasButtonGroupSelectionChanged(app, event)
            selectedButton = app.ModelBiasButtonGroup.SelectedObject;
            switch selectedButton
                case app.MbiasLow
                    app.comb(1)=1;
                case app.MbiasMed
                    app.comb(1)=2;
                case app.MbiasHigh
                    app.comb(1)=3;
            end
            combineuc(app)
            calcEDMF(app)
            resmin(app)
            updateplot(app)
        end
        % Selection changed function: SurrogateModelErrorButtonGroup
        function SurrogateModelErrorButtonGroupSelectionChanged(app, event)
            selectedButton = app.SurrogateModelErrorButtonGroup.SelectedObject;
            switch selectedButton
                case app.SurrLow
                    app.comb(3)=1;
                case app.SurrMed
                    app.comb(3)=2;
```

```
                case app.SurrHigh
                    app.comb(3)=3;
            end
            combineuc(app)
            calcEDMF(app)
            resmin(app)
            updateplot(app)
        end
        % Value changed function: Switch
        function SwitchValueChanged(app, event)
            updateplot(app)

            if strcmp(app.Switch.Value,'Combined Uncertainty')
                app.TextArea.Visible='off';
            else
                app.TextArea.Visible='on';
                app.TextArea.Position=[150 45 700 130];

            end
        end
        % Selection changed function:
        % VehiclePositionUncertaintyButtonGroup
        function VehiclePositionUncertaintyButtonGroupSelectionChanged(app, event)
            selectedButton = app.VehiclePositionUncertaintyButtonGroup.SelectedOb-
ject;
            switch selectedButton
                case app.VehicleLow
                    app.comb(2)=1;
                case app.VehicleMed
                    app.comb(2)=2;
                case app.VehicleHigh
                    app.comb(2)=3;
            end
            calcEDMF(app)
            resmin(app)
            updateplot(app)
        end
    end
    % App initialization and construction
    methods (Access = private)
        % Create UIFigure and components
        function createComponents(app)
            % Create UIFigure
            app.UIFigure = uifigure;
            app.UIFigure.Position = [100 100 971 625];
            app.UIFigure.Name = 'UI Figure';
            % Create UIAxes
            app.UIAxes = uiaxes(app.UIFigure);
            xlabel(app.UIAxes, 'X')
            ylabel(app.UIAxes, 'Y')
            app.UIAxes.FontName = 'Times New Roman';
            app.UIAxes.Position = [1 181 539 343];
            % Create Label
            app.Label = uilabel(app.UIFigure);
```

```
            app.Label.FontSize = 14;
            app.Label.Position = [568 342 25 18];
            app.Label.Text = '';
            % Create Label_2
            app.Label_2 = uilabel(app.UIFigure);
            app.Label_2.FontSize = 14;
            app.Label_2.Position = [579 264 25 18];
            app.Label_2.Text = '';
            % Create Switch
            app.Switch = uiswitch(app.UIFigure, 'slider');
            app.Switch.Items = {'EDMF vs BMU', 'Combined Uncertainty'};
            app.Switch.ValueChangedFcn = createCallbackFcn(app, @SwitchValue-
Changed, true);
            app.Switch.FontSize = 20;
            app.Switch.Position = [218 544 45 20];
            app.Switch.Value = 'EDMF vs BMU';
            % Create ModelBiasButtonGroup
            app.ModelBiasButtonGroup = uibuttongroup(app.UIFigure);
            app.ModelBiasButtonGroup.SelectionChangedFcn = createCallbackFcn(app,
@ModelBiasButtonGroupSelectionChanged, true);
            app.ModelBiasButtonGroup.TitlePosition = 'centertop';
            app.ModelBiasButtonGroup.Title = 'Model Bias';
            app.ModelBiasButtonGroup.FontSize = 20;
            app.ModelBiasButtonGroup.Position = [548 440 473 84];
            % Create MbiasLow
            app.MbiasLow = uitogglebutton(app.ModelBiasButtonGroup);
            app.MbiasLow.Text = 'Low -  [-2%  5%]';
            app.MbiasLow.FontSize = 14;
            app.MbiasLow.Position = [8.5 5 133 27];
            app.MbiasLow.Value = true;
            % Create MbiasMed
            app.MbiasMed = uitogglebutton(app.ModelBiasButtonGroup);
            app.MbiasMed.Text = 'Medium - [-2%  10%]';
            app.MbiasMed.FontSize = 14;
            app.MbiasMed.Position = [148.5 5 165 27];
            % Create MbiasHigh
            app.MbiasHigh = uitogglebutton(app.ModelBiasButtonGroup);
            app.MbiasHigh.Text = 'High - [-2%  15%]';
            app.MbiasHigh.FontSize = 14;
            app.MbiasHigh.Position = [324.5 5 141 27];
            % Create VehiclePositionUncertaintyButtonGroup
            app.VehiclePositionUncertaintyButtonGroup = uibuttongroup(app.UIFig-
ure);
            app.VehiclePositionUncertaintyButtonGroup.SelectionChangedFcn = cre-
ateCallbackFcn(app, @VehiclePositionUncertaintyButtonGroupSelectionChanged, true);
            app.VehiclePositionUncertaintyButtonGroup.TitlePosition = 'centertop';
            app.VehiclePositionUncertaintyButtonGroup.Title = 'Vehicle Position
Uncertainty';
            app.VehiclePositionUncertaintyButtonGroup.FontSize = 20;
            app.VehiclePositionUncertaintyButtonGroup.Position = [548 327 473 84];
            % Create VehicleLow
            app.VehicleLow = uitogglebutton(app.VehiclePositionUncertaintyBut-
tonGroup);
            app.VehicleLow.Text = 'Low -  [0%  1%]';
```

```
            app.VehicleLow.FontSize = 14;
            app.VehicleLow.Position = [12 5 128 27];
            app.VehicleLow.Value = true;
            % Create VehicleMed
            app.VehicleMed = uitogglebutton(app.VehiclePositionUncertaintyBut-
tonGroup);
            app.VehicleMed.Text = 'Medium - [0%  3%]';
            app.VehicleMed.FontSize = 14;
            app.VehicleMed.Position = [161.5 5 151 27];
            % Create VehicleHigh
            app.VehicleHigh = uitogglebutton(app.VehiclePositionUncertaintyBut-
tonGroup);
            app.VehicleHigh.Text = 'High - [0%  5%]';
            app.VehicleHigh.FontSize = 14;
            app.VehicleHigh.Position = [332.5 5 127 27];
            % Create SurrogateModelErrorButtonGroup
            app.SurrogateModelErrorButtonGroup = uibuttongroup(app.UIFigure);
            app.SurrogateModelErrorButtonGroup.SelectionChangedFcn = create-
CallbackFcn(app, @SurrogateModelErrorButtonGroupSelectionChanged, true);
            app.SurrogateModelErrorButtonGroup.TitlePosition = 'centertop';
            app.SurrogateModelErrorButtonGroup.Title = 'Surrogate Model Error';
            app.SurrogateModelErrorButtonGroup.FontSize = 20;
            app.SurrogateModelErrorButtonGroup.Position = [549 207 473 84];
            % Create SurrLow
            app.SurrLow = uitogglebutton(app.SurrogateModelErrorButtonGroup);
            app.SurrLow.Text = 'Low -  [-15%  10%]';
            app.SurrLow.FontSize = 14;
            app.SurrLow.Position = [8.5 7 135 25];
            app.SurrLow.Value = true;
            % Create SurrMed
            app.SurrMed = uitogglebutton(app.SurrogateModelErrorButtonGroup);
            app.SurrMed.Text = 'Medium - [-20%  15%]';
            app.SurrMed.FontSize = 14;
            app.SurrMed.Position = [160 7 156 25];
            % Create SurrHigh
            app.SurrHigh = uitogglebutton(app.SurrogateModelErrorButtonGroup);
            app.SurrHigh.Text = 'High - [-25%  20%]';
            app.SurrHigh.FontSize = 14;
            app.SurrHigh.Position = [329 7 134 25];
            % Create TextArea
            app.TextArea = uitextarea(app.UIFigure);
            app.TextArea.HorizontalAlignment = 'center';
            app.TextArea.FontSize = 16;
            app.TextArea.BackgroundColor = [0.9412 0.9412 0.9412];
            app.TextArea.Position = [123.671875 66 271 93];
        end
    end
    methods (Access = public)
        % Construct app
        function app = Venoge
            % Create and configure components
            createComponents(app)
            % Register the app with App Designer
            registerApp(app, app.UIFigure)
```

```
            % Execute the startup function
            runStartupFcn(app, @startupFcn)
            if nargout == 0
                clear app
            end
        end
        % Code that executes before app deletion
        function delete(app)
            % Delete UIFigure when app is deleted
            delete(app.UIFigure)
        end
    end
end
```

Developed using Matlab's app designer